#3

IOP PUBLISHING SUPERCONDUCTOR SCIENCE AND TECHNOLOGY
Supercond. Sci. Technol. 23 (2010) 073001 (20pp) doi:10.1088/0953-2048/23/7/073001

TOPICAL REVIEW

An overview on iron based superconductors

P M Aswathy, J B Anooja, P M Sarun and U Syamaprasad[1]

National Institute for Interdisciplinary Science and Technology (CSIR), Trivandrum- 695019, India

E-mail: syamcsir@gmail.com

See marked passages * and pictures

Received 16 March 2010, in final form 6 May 2010
Published 24 June 2010
Online at stacks.iop.org/SUST/23/073001

Abstract

The discovery of superconductivity at relatively higher temperatures in a non-cuprate system, $LnFeAsO_{1-x}F_x$ (Ln = lanthanides) has created tremendous activity among the reseachers in this field. This review is an overview on the present status and the future scope for iron pnictides. The various structural categories of iron based superconductors, the structural aspects, different preparation techniques of the material and the necessity for its optimization are discussed. The highlighting features of iron pnictide, i.e. the very high upper critical field, moderate magneto-transport and thermal properties, are also included. The article gives a summary of the prevailing arguments of researchers to relate the material to cuprates and also the comparative features of classical and MgB_2 superconductors. The existing challenges, such as optimizing synthesis methods for technological applications and clarifying the ambiguity in the superconducting mechanism and the flexibility of the material for any site substitution, will keep iron based superconductors on the frontiers of research for a long time, in parallel to HTS.

(Some figures in this article are in colour only in the electronic version)

Contents

[1] Author to whom any correspondence should be addressed.

1. Introduction

Since the discovery of superconductivity in mercury, solid state physicists have worked meticulously to attain superconductivity at technically relevant and feasible temperatures. Even a minor increase in the superconducting temperature can greatly ease the practical handling and application of superconductors. This necessity initiated strenuous effort in developing a superconductor above the BCS limit. The term 'high temperature superconductor' (HTS) was first coined for a family of cuprate-perovskite ceramic materials, discovered by Muller and Bednorz in 1986 [1]. The superconducting mechanism and theories supporting the phenomenon in HTS are still hot topics

of research. As the transition temperatures are much higher than the boiling point of liquid nitrogen, these materials have tremendous potential in commercial applications. The discovery of superconductivity in an intermetallic MgB_2 ($T_c = 39$ K) in 2001 also spurred renewed interest due to its potential in magnetic applications [2].

The superconducting world was reignited when Japanese researchers led by Hideo Hosono discovered a new class of iron based superconducting material having transition temperatures relatively higher than the conventional low temperature superconductors [3]. The team was primarily aiming at the fabrication of transparent oxide semiconductors for flat panel displays. They expected intriguing electromagnetic properties from the two-dimensional electronic structure of the compound LaT_MPnO (T_M-transition metal, Pn-pnictogen), known as oxypnictides. Research on iron based superconductors was taken up seriously only after the discovery in 2006 of superconductivity at 4 K in LaOFeP, a member of this oxypnictide family [4]. The T_c climbed up to 26 K with the replacement of phosphorous by another pnictogen, arsenic and some oxygen atoms with fluorine [3]. The discovery tantalized physicists and materials scientists into a renewed frenzy of activity, since the compound contained the most familiar ferromagnetic atom 'iron' which does not mix with superconductivity. A great deal of work is in progress to explore the similarities with HTS and thereby to pave the way towards the superconducting mechanism behind the unconventional high temperature superconductors.

One of the exciting aspects of these new superconductors is that they belong to a comprehensive class of materials where many chemical substitutions are possible. This versatility has already opened up new research avenues to understand the origin of the superconductivity, and should also enable the superconducting properties to be tailored for commercial technologies. Every week, scientists are posting papers on the preprint server arXiv with new proclamations of the material properties. The only problem working with iron based superconductors is the trickier chemistry of the compound and the toxicity and volatility of arsenic.

2. Preparation techniques

Different synthesis methods have been used for the Fe based superconductors $LnFeAsO_{1-x}F_x$ (Ln = lanthanides) by many research groups. The synthesis methods can be divided into three groups: (1) the solid state reaction method (2) the high pressure synthesis method and (3) the flux method. The first two methods are mainly used for the preparation of polycrystalline samples, while the flux method is widely used for synthesizing single crystals. Recently wire and film forms have also been reported [5–9].

2.1. Solid state method

The solid state reaction method, also known as the ambient pressure method, was the widely used technique starting from the first reported iron based superconductor by Kamihara *et al* [3]. Generally $LnFeAsO_{1-x}F_x$ samples were prepared by taking LnAs, FeAs, Fe_2As, LnF_3, and rare earth oxides as starting materials. LnAs is obtained by reacting Ln and As at 500–900 °C for 12–24 h in a silica tube filled with argon gas. Later, $LnFeAsO_{1-x}F_x$ samples were obtained by stoichiometric mixing of the starting materials and sintering at 1150–1250 °C for 40–60 h in sealed quartz tube [3, 10, 11]. Considering the high vapour pressure of elementary As at 600 °C, the synthesis of the As compounds as the precursor was required to avoid the explosion of the sealed glass sample during the main reactions [12]. All the above processes, including cutting, weighing and grinding (except annealing) are done within a glove box filled with inert gas (Ar gas has been commonly used) to avoid oxidation of the rare earth metals as well as problems due to arsenic toxicity. In some reports, during the first step of the synthesis of $LnFeAsO_{1-x}F_x$, Ln, Fe and As powders were mixed in the ratio of 1:3:3 [11, 13]. Some impurity phases were reported in all these synthesis methods and influenced the superconducting properties of the samples. Chen *et al* [14] used Fe_2O_3 as a source of oxygen instead of using rare earth oxides, because of its high stability. They prepared $LnFeAsO_{1-x}F_x$ using LnAs, Fe_2O_3, Fe and LaF_3 as starting materials. No obvious foreign phases were detected in this method [14, 15]. To improve the densification, the $LnFeAsO_{1-x}F_x$ samples prepared were again ground and sintered at a higher temperature (1300 °C) [16, 17].

2.2. High pressure method

The high pressure method (HP) is more efficient than the ambient pressure (solid state) method for the synthesis of gas releasing compounds such as $LnFeAsO_{1-x}F_x$ at high temperatures [18–20]. Severe fluorine loss observed in the common vacuum quartz tube seal method can thus be avoided. A short sintering period, effective maintenance of fluorine in high pressure capsule, etc make the HP method superior to solid state synthesis. Generally, in the HP method stoichiometric amounts of starting materials were mixed well, ground thoroughly and pressed into pellets. The pellets were sealed in boron nitride crucibles and sintered under a pressure of 6 GPa at 1250 °C for 2 h. The short sintering times led to the formation of impurity phases such as rare earth oxides, arsenides and fluorides, and is a disadvantage.

The HP technique drastically improves the superconducting transition temperature. For example T_cs of $LaFeAsO_{1-x}F_x$ and $SmFeAsO_{0.85}F_{0.15}$ have been increased up to 41 K and 55 K respectively; higher than those reported by AP synthesis ($T_c = 26$ K, 52 K respectively) [18, 19]. Yang *et al* [19] has done a comparative study of AP and HP methods on Sm based samples. Higher T_c, smaller lattice parameters and unit cell volume were observed in high pressure synthesized samples. These results indicate that HP synthesis is advantageous over the quartz tube method in better substituting F^- for O^{2-} by eliminating the volatilization of F^-. XRD patterns of the samples show that the diffraction peaks of the HP nominal sample shift to higher diffraction angle compared to those of the AP sample, indicating lattice shrinkage due to doping. Moreover, it is the only successful method to synthesize good quality oxygen deficient oxypnictide samples. The high pressure method

also raises the percentage of fluorine doping, as high as 60% in $LaFeAsO_{0.4}F_{0.6}$, which is six times higher than the ambient pressure method (10%) [18, 20]. Heavy rare earth elements such as Tb, Dy etc can induce superconductivity above 40 K by using the HP method [21]. The T_c of these materials is comparable to that of the light rare earth based compounds synthesized by the solid state reaction. But it was demonstrated that ambient pressure sintering of $NdFeAsO_{0.75}F_{0.25}$ by controlling As vapour, yields a higher $T_c = 55$ K than HP sintering. It has been also shown that spark plasma sintering densification is an effective way of compacting the oxypnictide powders with a theoretical density >95% resulting in superconducting properties better than HP synthesized samples and almost similar to single crystals of the same material [22].

2.3. Flux method

In order to tailor the intrinsic properties of iron based superconductors, single crystal formation using the flux method was chosen [23, 24]. The first report based on this method was from Jia *et al* [23]. They have synthesized single phase samples of $NdFeAsO_{0.82}F_{0.18}$ with plate like crystals of size ranging from 5 to 50 nm. In the preparation process, NaCl/KCl was used as the flux, with a mass ratio NaCl:NdFeAs(O, F) = 10:1, and sealed in an evacuated quartz tube, and heat treated at 1050 °C for 10 days. This method is efficient in lowering the processing temperature, and growing high quality single crystals, even though the growth time is longer. Optimized methods for preparing large crystals may be suggested in the future. The flux and high pressure sintering methods are found to be more effective for synthesis of good quality superconductors of this category [25–28].

2.4. Wire and film preparation

The relatively high T_c and extremely large H_{c2} make iron based superconductors promising candidates for technological applications. But these applications require the superconductors in wire and film forms. Wire forms of iron oxypnictides were recently reported by a group in the Key Laboratory of Applied Superconductivity, China and the first report was on a La based system [5, 9]. They used the powder-in-tube (PIT) method for their preparation [5, 6, 9]. The raw materials were ground and filled into an Fe tube. A titanium sheet was inserted inside the tube in order to prevent reaction between the raw materials and the Fe tube. After packing, the tube was rotary swaged and then drawn into wires. The wires were cut into pieces, sealed in a Fe tube and reacted at 1150 °C for 40 h to get the final product. Obviously, a suitable sheath material which does not degrade the superconducting properties is a necessity. The effect of various sheath materials such as Fe/Ti, Ta, Nb on the microstructure and superconducting properties of iron pnictides was studied by the same group [29]. Nb was the best among these in terms of reactivity, J_c and T_c. However, the presence of impurities and voids, the weak links between the grains, and the hard, brittle nature of this material poses many challenges in the fabrication of wires with the desired geometry.

Epitaxial thin films are another form in which it is essential to explore the intrinsic properties of the superconductors. Successful fabrication of thin films is essential for the development of electronic devices such as the Josephson device and SQUIDS. Actually, it is a tough task to obtain even polycrystalline films because of the difficulties associated with the excitation laser source and the preferential deposition of non-metallic impurity phases present in iron oxypnictides. Some groups, mainly Hosono *et al* and Backen *et al*, succeeded in the fabrication of epitaxial thin films by pulsed laser deposition (PLD) [7, 8, 30–33]. The first report is on Co-doped $SrFe_2As_2$ on (100) mixed perovskite (La, Sr)(Al, Ta)O_3 single crystal substrates using a second harmonic Nd:YAG laser. Just after that the thin film forms of $LaFeAsO_{1-x}F_x$ on (001)-oriented $LaAlO_3$ and MgO were developed by a group in Germany [30]. The T_c of the film sample was comparable to that of the bulk value for the former, but a reduced T_c was seen in the latter case which is attributed to excess oxygen content.

3. Structural properties

3.1. Crystal structure

The iron based superconductors that have been reported so far can be categorized into four major classes according to their structure. The first among these is LnFeAsO; known as '1111' type (Ln represents lanthanides). LnFeAsO has a ZrCuSiAs type structure belonging to the tetragonal $P4/nmm$ space group. It is a stack of alternating positively charged Ln–O layers and negatively charged Fe–As layers along the c-axis. The Ln_2O_2 layer is an insulating charge reservoir layer, while the Fe_2As_2 layer acts as the conducting active block. The structure of LnFeAsO comprises sheets of Fe^{2+} ions in between ionic blocks of $LnOAs^{2-}$. The Ln atoms (having $4mm$ site symmetry) are coordinated by four As atoms and four O atoms forming distorted square antiprisms. The Fe atoms ($42m$) form square nets perpendicular to the c-axis.

The transmission electron microscope (TEM) images and fast Fourier transform (FFT) [10] calculated diffraction patterns depict the layered structure which can be seen in figure 1. The parent compound LnFeAsO is not superconducting, rather it is an antiferromagnetic (AFM) semimetal [34]. On cooling LnFeAsO, the resistivity as well as magnetic susceptibility variations with respect to temperature show an anomaly near 150 K. This anomaly includes a structural phase transition followed by antiferromagnetic long range ordering, which was studied using neutron magnetic scattering. The structural phase transition, i.e. from the tetragonal $P4/nmm$ to the orthorhombic $Cmma$ space group [35] is found to be at a temperature $T_S = 160$ K, but the onset of the transition is at around 180–200 K [36]. The Jahn–Teller effect is suspected as one of the candidates that drives this structural distortion. On increasing the internal chemical pressure by substituting the Ln site with rare earths having lower ionic radii, the temperature of the structural transition T_S in parent undoped compounds is found to be reduced considerably. This in turn favours the enhancement of T_c which shows that the normal striped orthorhombic $Cmma$ phase competes with the superconducting tetragonal phase. It also leaves a possibility to push the temperature of the stripe

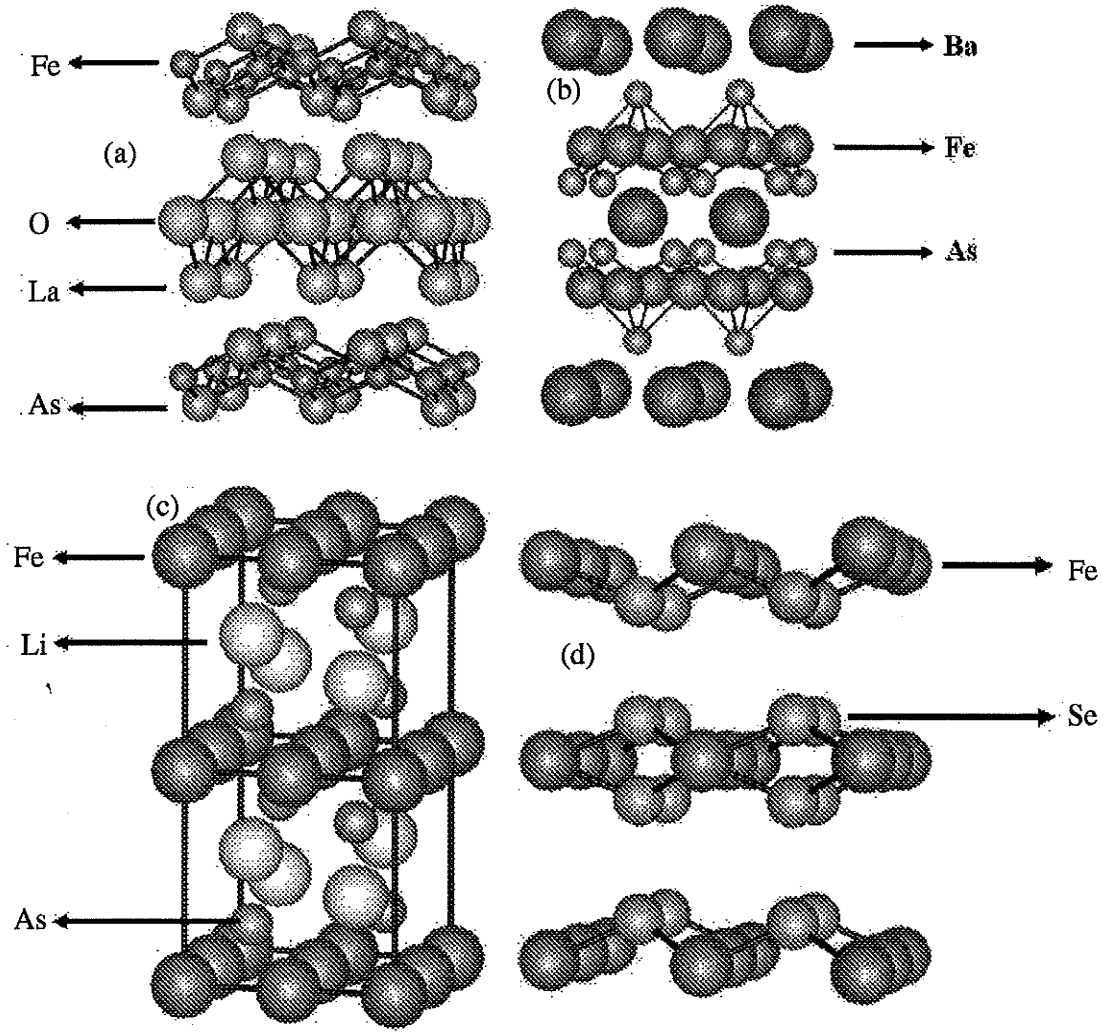

Figure 1. Crystal structure of the four categories of iron pnictides (a) '1111' type (b) '122' type (c) '111' type (d) '11' type.

phase towards zero so as to achieve a superconductor with a much higher T_c [37]. Doping the parent compound leads to suppression of the tetragonal to orthorhombic crystallographic phase transition with the onset of superconductivity. Although there are many reports on the complete suppression of the structural phase transition, a high resolution synchrotron x-ray diffraction study on $SmFeAsO_{1-x}F_x$ displays the survival of the orthorhombic symmetry through the metal–superconductor boundary well into the superconducting region [38]. Moreover, the crystal symmetry crossover coincides with the reported drastic anomalies in resistivity, Hall coefficient and pressure coefficient of T_c, which elucidates the role of the low temperature crystal structure in the electronic properties of these superconductors.

Although x-ray diffraction gave ideas about the overall crystal structure, the experimental data on the local structure of iron pnictides using extended x-ray absorption fine spectrum (EXAFS) provided the key information regarding the electron–lattice interaction at the onset of superconductivity in oxypnictides [39]. Both As and Fe k edge EXAFS in doped as well as undoped LaFeAsO systems reflected lattice instability as local distortions which are of electronic origin (different from the crystallographic phase transition). The upturn in the temperature dependence of mean square relative displacement (MSRD) in the F doped LaFeAsO system below 70 K is attributed to the splitting of Fe–As bonds into elongated and shortened Fe–As bond distances. The anomaly also reveals a certain polaron formation well above T_c. Studies on the same compound were also reported by Tyson *et al* [40]. Here, the Fe–As and Fe–Fe bonds, well modelled by Einstein type pair correlations, displayed no low temperature anomalies. For Fe–As bonds, the Einstein temperature was identical for both doped and undoped samples, while the doping caused an increase in the Einstein temperature for the Fe–Fe correlation. The inferences were consistent with the magnetic origin of superconductivity as proposed by some earlier reports. Though the above results are on the same system Iadecola *et al* has attempted a local structure analysis on different '1111' compounds with rare earths of varying ionic radii [41]. On comparing the inter-atomic distances and

MSRD using EXAFS, the highly covalent nature of the Fe–As bond, and the systematic change in the Fe–Fe and Fe–Ln atomic correlations were observed, corresponding to ionic radii change in Ln. The results suggested that Fe–Ln phonon modes contribute in correlating magnetism and superconductivity. While local structure analysis of the '1111' system was studied using EXAFS, the electronic structure of the '111' system was analysed using resonant and non-resonant x-ray emission spectrum at the Fe $L_{2,3}$ edges [42]. The studies concluded that the energy and ratio of intensities share similar trends with the rest of the FeAs systems proposing iron pnictides as a weakly or moderately correlated system.

The Ln–As distance and Fe–As–Fe angle are suggested as two crucial parameters to be controlled to enhance superconductivity [43]. Shirage *et al* revealed that the *a*-axis length, corresponding to the distance between Fe atoms in the square lattice, also has a strong correlation with T_c in the '1111' system [44]. It was found that the systematic replacement of Ln from La to Ce, Pr, Nd and Sm in $LnFeAsO_{1-y}$ resulted in a gradual decrease in the *a*-axis lattice parameter and a corresponding increase in T_c [43]. The T_c in $LnFeAsO_{1-y}$ is strongly dependent on tetrahedral distortion of the As–Fe–As bond angle [45] and the highest T_c is obtained when As–Fe–As forms a regular tetrahedron. The exchange couplings (J_1 and J_2) and the electronic bandwidth (W) are found to be directly related to the As–Fe–As angle which supports the role of electronic correlations in superconductivity [46, 47]. The ratio of effective Coulomb interaction (U) to electronic bandwidth (W) increases for high T_c iron pnictides with comparable U value. It is generally seen that the Fe–As distance is around 0.24 nm; As–Fe–As angles are either 107.5° or 113.5° for the '1111' system (changes with composition), almost regular, i.e. close to 109.47° in the '122' system [48], while it is elongated in the '111' system [49]; and the Fe–Fe distance on a square lattice is around 0.285 nm (the values may change slightly as samples change). A correlation was established between T_c and the positions of Fe atoms next to the doping element position which was in good agreement with all high temperature superconductors. The study concluded a common resonance mechanism between the de Broglie wavelength of charge carriers and the directions in the crystal lattice [50].

The second category, AFe_2As_2, has a $ThCr_2Si_2$ structure abbreviated as '122' type. Here the A site corresponds to a divalent ion (A = Ba, Sr, Ca). The AFe_2As_2 structure was first reported in $BaFe_2As_2$, which displayed antiferromagnetic ordering similar to '1111' type [25]. The third one has the Cu_2Sb type structure ('111' type) and was first reported in superconducting LiFeAs. Superconductivity in LiFeAs is extremely sensitive to sample preparation [27, 51, 52]. The last category is the simplest one among iron based superconductors having a α-PbO type structure ('11' type). It was first reported in α-FeSe [28]. Another category among iron based superconductors, known as iron arsenide fluorides AFeAsF (A = Sr, Ba, etc), also have the ZrCuSiAs structure [53–56].

Recently many new layered compounds composing both antifluorite pnictide layers and perovskite oxide layers such as Ti doped $Fe_2As_2(Sr_3Sc_2O_5)$ (T_c = 45 K), $Fe_2P_2(Sr_4Sc_2O_6)$ (T_c = 17 K), $(Fe_2As_2)(Sr_4V_2O_6)$ (T_c = 37.2 K), and cobalt substituted $(Fe_2As_2)(Sr_4MgTi_{0.6})$ (T_c = 26 K which ramps up to 46 K on applying 4 GPa pressure), were reported [57–60].

3.2. Electronic structure

The electronic structure of LnFeAsO has been proposed by several groups after performing *ab initio* calculations of the band structure using density functional theory (DFT) [35, 61]. The Fermi surface (FS) of iron based superconductors was studied both theoretically and experimentally [61–63]. It has been reported that the FS of LaFeAsO resembles that of LaFePO [63] to some extent. One of the first principles band structure calculations concludes that the Fermi surface consists of two hole pockets and two electron pockets which are well exhibited by a minimal two band model proposed by Raghu *et al* [64]. The states near the Fermi level are dominated by Fe 3d states lightly mixed with As p states [61]. These Fe d_z states hybridize with As p states and yields a heavy 3D pocket in addition to the two hole and two electron pockets. The DFT and dynamical mean field theory calculations done on LaFeAsO predict a steep and negative slope of density of states (DOS) at the Fermi level [65]. Moreover, the FS has an instability of magnetic order, which seems to be a collinear antiferromagnet, associated with a nesting of (π, π) wavevectors. Different experiments such as neutron magnetic scattering [66, 67], quantum oscillation measurements [68–70], angle resolved photoemission spectroscopy (ARPES) [71–75] and angular magneto-resistance measurements have been done to probe the FS of iron pnictides [76]. Early reports on local density approximation (LDA) calculations also suggest that the spin density wave (SDW) results from FS nesting between the hole-like FS at Γ and the electron-like FS at X [77–79].

The ARPES measurements on hole doped $BaFe_2As_2$ crystals observed three FS sheets: an inner hole-like FS pocket, an outer hole-like FS pocket (both centred at the Brillouin zone centre) and a small electron-like FS [73, 80–84]. A fourth FS is also proposed by Nakayama *et al* [83]. It is also reported that heavily electron doped '122' systems have only an electron-like FS without superconductivity, which supports inter-FS superconductivity [85]. The fluctuation exchange approximation (FLEX) using the five band Hubbard model has been used in explaining the decrease in nuclear relaxation rate and susceptibility upon cooling, as due to the existence of a high DOS near the Fermi level for the '1111' system in contrast to hole doped '122' systems where we see an increase of the nuclear relaxation rate with doping [86]. The comparison of normal state and superconducting properties in these systems supports the FS nesting. While the FLEX employed with an effective four orbital shows a FS which does not favour the stripe-like antiferromagnetic order. It also discards the pairing interaction and suggests that exchange interaction between local moments of Fe 3d orbitals plays a crucial role [87].

The '122' family is predicted to have a more pronounced 3D electronic structure than the '1111' family from the LDA band structure calculations [73, 88–90]. The fairly high T_c values in the '122' family suggests that high temperature

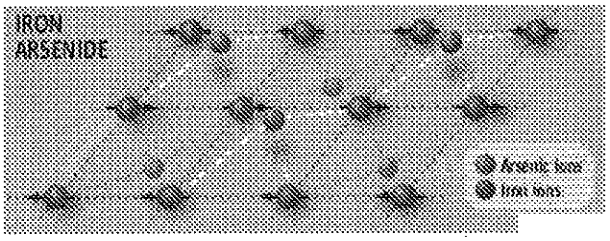

Figure 2. The magnetic structure of iron pnictide.

superconductivity does not just exist in systems with low dimensional electronic structures such as cuprates. A 3D to 2D transition has also been observed at temperatures above the structural transition temperature, T_S in the '122' system [90]. But the relationship between three dimensionality and relatively high T_c needs to be clarified.

3.3. Magnetic structure

The close proximity of AFM and superconductivity in the phase diagram prompted an extensive study to clear the possibility of magnetically mediated superconductivity [91] in terms of localized spins, itinerant electrons, etc. Various theoretical calculations based on (a) strong coupling (J_1–J_2 model) [46, 92, 93] (b) weak coupling [94–98] and (c) moderate correlations [99, 100] were proposed.

The magnetic structure of the oxypnictides within the a–b plane consists of chains of parallel Fe spins that are coupled antiferromagnetically in the orthogonal direction with an ordered moment of less than 1 μ_B (in NdFeAsO it is found to be minimum = 0.25 μ_B). The observed magnetic moment per iron atom was much smaller than the theoretically predicted one (2.3 μ_B) which is supposed to be due to magnetic frustration and/or spin fluctuations [46, 47, 66]. The typical spin alignment in iron pnictides is shown in figure 2. The reduction in iron magnetic moment weakens the Fe–As bonding, and in turn increases As–As interactions, causing a decrease in the c-axis, leading to unconventional superconductivity [101]. The magnetic ordering is seen below 150 K, i.e. after structural distortion [66, 102]. Moreover, in LnFeAsO compounds (except Ln–La), the rare earth 4f electrons form local moments rather than hybridizing with Fe 3d electrons [103, 104], but there are reports supporting the hybridization [105, 106]. The ^{139}La-NMR experiment gives the correlation between magnetic ordering and structural distortion on cooling [107]. The effect of structural change is induced mainly due to the reorientation of Fe 3d spins which can be suppressed by doping [35]. Doping reduces the degree of Fermi surface nesting and in turn suppresses the magnetic instability. Neutron scattering studies on Ce based iron oxypnictide show an orientational relationship between the magnetic alignment and lattice distortion. The iron magnetic moment spins are stripe-like but are parallel to c-axis and have double the magnitude in contrast to LaFeAsO which are supposed to be due to strong coupling or magnetic interaction between Ce and Fe moments [43]. The '122' systems show a simultaneous tetragonal-to-orthorhombic transition at about

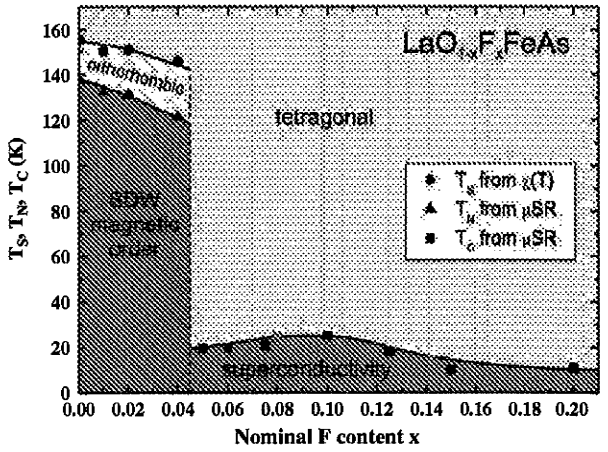

Figure 3. Electronic phase diagram of $LaFeAsO_{1-x}F_x$. The doping dependence of the magnetic and superconducting transition temperatures determined from the μSR experiments. Also shown are the tetragonal-to-orthorhombic structural transition temperatures T_S determined directly from x-ray diffraction and from susceptibility measurements, which show a kink and subsequent strong reduction below T_S. Reprinted by permission from MacMillan Publishers Ltd: *Nature Materials* [108], copyright 2009.

140 K, with the onset of q = (101) AFM order having a magnetic moment of 0.87 μ_B per iron in $BaFe_2As_2$ along the a-axis of the ab planes, unlike '1111' systems [67]. Moreover, the magnetic order of the '122' system is supposed to have a multiorbital nature.

4. Enhancement of critical temperature

4.1. Doping effect

The phase diagram of iron pnictides depicted so far is approximately symmetric against hole doping and electron doping, which can be seen in figure 3. Both electron doping at an oxygen site and hole doping at a lanthanide site, was tried first. The T_c shows a trapezoidal dependence on F content, with the highest T_c = 26 K in $LaFeAsO_{1-x}F_x$ at 5–11 at.% doping. Fluorine doping helps increase the electron density in the conduction layer without affecting the geometry of the FeAs layer. On lowering the temperature, the F doped iron based superconductor displays a crystallographic transition. The lattice constants decrease systematically with nominal dopant concentration, indicating the inner chemical pressure. The distance between $(LaO)^{\delta+}$ and $(FeAs)^{\delta-}$ layers prominently decreases by F doping, suggesting that the electron doping enhances polarization and Coulomb interaction between the layers [35]. F doping suppresses both the structural phase transition and AFM order [66]. Mossbauer spectroscopy, muon spin resonance, neutron scattering and transport experiments done on different $LnFeAsO_{1-x}F_x$ samples also support this [108]. The temperature dependence of resistivity in non-superconducting LnFeAsO compounds as well as their optimally fluorine doped compounds are shown in (figures 4(a) and (b)). The ρ–T graph of the parent compounds show an anomaly around T_S = 150 K associated with the SDW

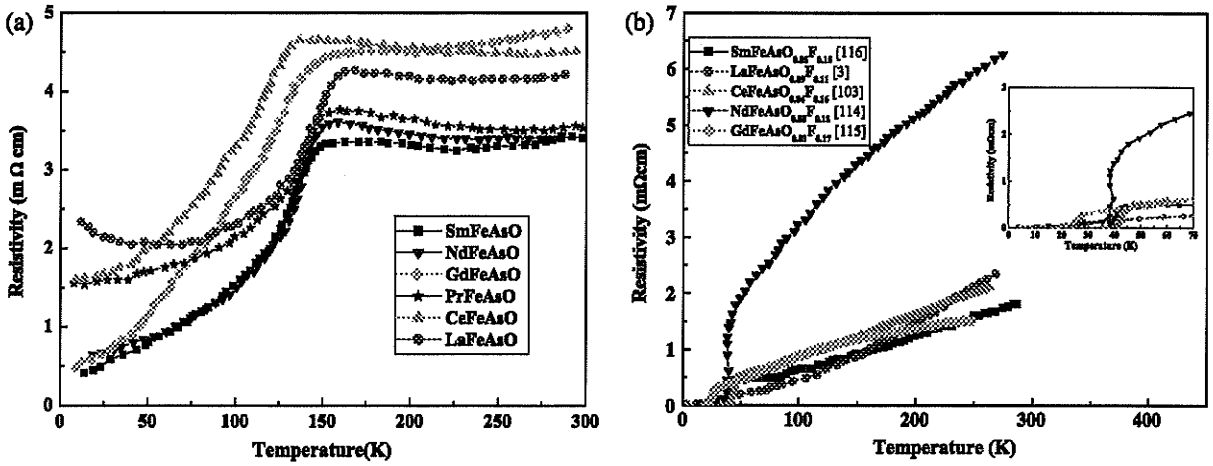

Figure 4. Temperature dependence of resistivity in (a) LnFeAsO [109] and (b) their F doped samples.

state, below which the resistivity drops steeply with a T-linear behaviour. Fluorine doping suppresses the SDW anomaly peak thereby shifting T_S to a lower temperature that switches over to a superconducting transition at optimum doping. The ρ–T graphs of different '1111' compounds having lanthanides of varying ionic radii (Ln–La, Ce, Sm, Nd, and Gd) with optimum fluorine doping have been plotted. All the ρ–T plots correspond to solid state synthesized samples at ambient pressures so that one can compare the effect of Ln ionic radii variation on T_c without the influence of any external pressure.

High temperature annealing causes evaporation loss of the F^- content which can be solved by high pressure synthesis. Therefore, high pressure synthesized F doped samples show even better superconducting properties than those synthesized by the ambient pressure method [18, 110, 111]. The F doping effect studied on $SmFeAsO_{1-x}F_x$ and $SmFeAsO_{1-y}$ revealed that F cannot substitute for O^{2-} in samples without oxygen vacancies [19]. The temperature dependence of the density of states in $SmFeAsO_{1-x}F_x$ investigated by Ou *et al*, exhibited a doping independent intrinsic pseudogap and spectral weight suppression at E_F which is supposed to be due to domain boundaries, inhomogeneities of fluorine dopant or oxygen vacancies [112]. The variation of T_c with respect to pressure, as well as doping concentration, were studied on almost all '1111' type superconductors [13, 113]. Both dT_c/dP and dT_c/dx gave the same sign, indicating the same suppression effect on the spin density wave state. It was also proposed that the maximum T_c possible in '1111' compounds is in the 50s K and the initial lower values are attributed to non-optimal synthesis.

The enhancement in T_c through doping at different sites was tried in all the categories of iron pnictides and is listed in table 1. Rare earth substitution at the Ln site was suggested as a route to enhanced T_c [114–116]. The substitution effect in $LnFeAsO_{1-x}F_x$ with Ln = Ce, Sm, Nd, Pr, Gd, Eu, Tm revealed that T_c increases to 41 K for Ce, 41–55 K for Sm, 50 K for Nd, 52 K for Pr and 36 K for Gd substitution. Eu and Tm substituted compounds could not achieve even the tetragonal ZrCuSiAs type structure, and hence the authors concluded that superconductivity can be attained only by iron oxypnictides having light rare earth elements. Rare earths with smaller ionic radii, decreased the lattice constants, thereby developing inner chemical pressure leading to higher T_c [35]. But heavy rare earth based iron oxypnictides also displayed high T_c by high pressure synthesis of the samples [21, 117]. Later, superconductivity was also reported for a heavy rare earth based '1111' system prepared by the solid state method, this has been included in the table 1. Doping brings structural modifications such as a reduction in cell volume, a decrease in distance between layers, an increase in distance between Re^{3+} and F^- which enhances spin and charge density fluctuations [19].

Several superconducting mixed rare earth oxypnictides were also reported. La doped iron oxypnictide $SmFeAs_{0.95}La_{0.05}O_{0.85}F_{0.15}$ exhibited a record T_c of 57.3 K [118]. A series of HP synthesized $La_{1-x}Sm_xFeAsO_{0.85}$ showed a monotonic increase of T_c from 31.2 to 55 K with increasing Sm doping (x = 0–1) [119]. Enhancement of T_c up to 47.5 K was seen in $Ce_{1-x}Gd_xFeAsO_{0.84}F_{0.16}$ as a consequence of internal pressure due to Gd substitution [120]. The effect of aliovalent dopants was reported by Che *et al* in the Ce doped series of $La_{1-x}Ce_xFeAsO_{0.9}F_{0.1}$ with T_c = 28.78 K, while the Pb doped series $La_{1-x}Pb_xFeAsO$ samples showed T_c around 10 K even without F doping [121].

Hole doping was first tried using Ca^{2+} ions in LaFeAsO at the lanthanide site and did not show superconductivity. Wen *et al* reported superconductivity in $La_{1-x}Sr_xFeAsO$ (T_c = 25 K) even in the absence of F doping [122]. This is attributed to the greater ionic radius mismatch between the La^{3+} ion and Ca^{2+} ion than with the Sr^{2+} ion. Hole doping also achieves superconductivity in AFe_2As_2 compounds by nominally substituting the A site with alkali metals such as potassium or sodium [26, 123]. The structural and magnetic transitions of $BaFe_2As_2$ begin to diminish with hole doping and superconductivity emerges in $Ba_{1-x}K_xFe_2As_2$ even with small potassium contents, and a maximum T_c of 38 K is obtained at x = 0.4. Superconductivity and antiferromagnetic ordering co-exists, at least in the underdoped region (x < 0.2), and a superconducting dome exists around (x = 0.4–0.5), which can be seen in the phase diagram (figure 5) [25, 124, 125].

Table 1. List of iron pnictides belonging to different categories and their corresponding critical temperatures [3, 12, 16, 21, 25–28, 53, 56, 64, 103, 114, 121–123, 126–159].

	Type of superconductor	Examples	Value of x	Synthesis method	$T_{c-onset}$ (K)
'1111'	$ReFeAs(O_{1-x}F_x)$	Re = La, Ce, Nd, Sm, Gd, Y, Eu	0.11, 0.16, 0.12, 0.2, 0.17, 0.1, 0.15	S.S.	26, 41, 50, 52, 36, 10, 11
		Re = La, Pr, Nd, Sm, Gd, Tb, Dy	0.6, 0.11, 0.11, 0.1, 0.2, 0.1, 0.1	H.P.	43, 52, 51.9, 55, 52, 46, 45
	$ReFeAs_{1-\delta}(O_{1-x}F_x)$	Re = La	0.1	S.S.	28.5
	$ReFeAsO_{1-x}$	Re = La, Ce, Pr, Nd, Sm, Gd, Tb, Dy, Ho and Y		H.P.	31.2, 46.5, 51.3, 53, 55, 53.5, 48, 52.2, 50.3, 46.5
	$(Re_{1-x}A_x)FeAsO$	(Gd/Tb, Th)(La, Pb)	0.2, 0.2	S.S.	56, 52, 10
		(La/Sr)(Pr/Sr), (Nd/Sr)	0.13, 0.25, 0.2	S.S.	25, 16.3, 13.5
	$Re(Fe_{1-x}A_x)AsO$	Re = La, Sm and A = Co	0.15, 0.1	S.S.	14.3, 15
		Re = La and A = Ni, Ir	0.4, 0.075	S.S.	6.5, 11.8
	$ReFe(As_{1-x}A_x)O$	Re = La, Sm and A = P	0.3, 0.565	S.S.	10.5, 4.1
	$A(Fe_{1-x}B_x)AsF$	A = Ca, Sr and B = Co	0.1, 0.125	S.S.	22, 4
	$(A_{1-x}B_x)FeAsF$	A = Sr and B = La, Sm	0.4, 0.5	S.S.	29.5, 56
		A = Ca and B = Nd, Pr	0.6, 0.6	S.S.	57.4, 52.8
'122'	$(A_{1-x}B_x)Fe_2As_2$	A = Ba, Sr and B = K	0.4	S.S	38
		A = Sr and B = Cs, K	0.6, 0.6	S.S	37, 37
		A = Eu and B = K, Na	0.5, 0.3	S.S.	32, 34.7
		A = Ca and B = Na	0.5	S.S.	20
	$A(Fe_{1-x}B_x)_2As_2$	A = Ba/Sr/Ca B = Cr, Mn, Cu			No superconductivity
		A = Ba and B = Co	0.2	S.S.,	22
		A = Ba and B = Ni, Pt, Rh, Pd	0.096, 0.1, 0.057, 0.053	Flux	20.5, 23, 24, 19
		A = Sr and B = Rh, Ir, Pd, Ru	0.25, 0.43, 0.15, 0.4	S.S.	21.9, 24.2, 8.7, 11.8
	$AFe_2(As_{1-x}B_x)_2$	A = Ba/Eu, B = P	0.32	S.S.	30, 26
'111'	AFeAs (A = Li, Na)	A = Li		S.S	18
		A = Na		S.S	9
		$Li_{1-x}FeAs$	0.2, 0.4	H.P.	16,18
'11'	α-FeSe			S.S	8
				H.P.	27
	$Fe(Se_{1-x}A_x)$	A = Te, S	0.5, 0.2	S.S	15.3, 15.5
	$(Fe_{1-x}A_x)Se$	A = Co, Ni	0.05	S.S	10
	FeTe			S.S	No superconductivity
	$Fe(Te_{1-x}A_x)$	A = S	0.2	S.S	10

The thorium ion was also chosen as a good candidate for substitution at the rare earth site in order to achieve an even higher T_c. $Gd_{1-x}Th_xFeAsO$ displayed a T_c of 56 K, which was much higher than the F doped $GdFeAsO_{1-x}F_x$ [136] sample. Later, partial substitution of Tb^{3+} by Th^{4+} in TbFeASO, exhibited superconductivity with a T_c of 52 K [117].

Cobalt is another widely used candidate for electron doping. Substitution of Co atoms at the Fe site in CaFeAsF induced superconductivity without creating localized moments [151, 160–162]. Doping at $(CaF)^{\delta+}$ exhibited a higher T_c = 22 K than 4–12% cobalt substituted LaFeAsO (T_c = 13 K) and SmFeAsO (T_c = 15 K) [53, 139, 161]. Cobalt has also been doped together with fluorine in '1111' systems, but resulted in the suppression of T_c [163]. Co doping in $SrFe_2As_2$ epitaxial thin films exhibited T_c = 20 K, which is the same as that of the polycrystalline bulk samples [7]. Rare earth doping at the A site in AFeAsF is also a means to higher T_c, even up to 56 K [56, 145].

An arsenic deficient iron based superconductor, $LaFeAs_{1-\delta}O_{0.9}F_{0.1}$ (T_c = 28.5 K), was also reported by Fuchs *et al* [133]. Recent reports show phosphorous doping at the arsenic site, attaining a maximum T_c of 30 K in '122' compounds [140, 156, 157] and below 11 K in the '1111' family of iron arsenides [140]. Moreover, non-magnetic impurity (Zn) doping was also investigated. It selectively affected the AFM order in the parent compound but did not help T_c enhancement in F doped samples [164]. Dopants such as Rh, Ir, Pd, Ni, Ru and Mn at the Fe site were tried to induce superconductivity in iron arsenides and most of them led to insensitive suppression of T_c, which stood against the proposed s-wave pairing symmetry [143, 152–155, 165]. Both doping at the Fe site and the creation of As vacancies reveal the fact that iron based superconductors can to some extent tolerate in-plane disorder in the FeAs conducting layer.

4.2. *Effect of oxygen deficiency and external pressure*

Ren *et al* [134] reported a series of F free oxygen deficient samples ($LnFeAsO_{1-y}$; Ln–Gd, Sm, Nd, Pr, Ce, La) prepared by the HP technique. Oxygen deficiency can produce more lattice shrinkage and charge carriers, thereby increasing the density of states (DOS). To investigate the effect of oxygen deficiency, $NdFeAsO_{1-y}$ [45] was studied for different oxygen vacancies. The study revealed that T_c increased abruptly to a

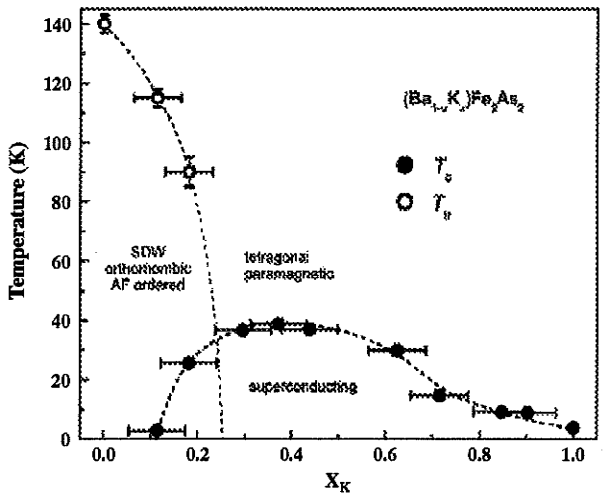

Figure 5. Phase diagram of $Ba_{1-x}K_xFe_2As_2$.

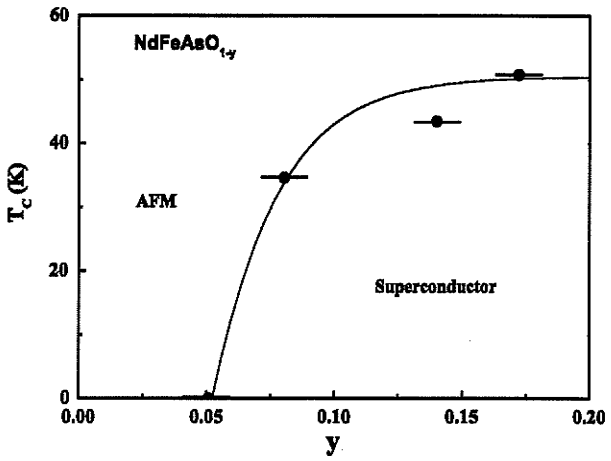

Figure 6. Phase diagram of oxygen deficient $NdFeAsO_{1-y}$ [45].

maximum with a slight doping of oxygen vacancies and then decreased with a further increase in oxygen vacancies, i.e. a dome shaped phase diagram was obtained as shown in figure 6.

The onset T_c values of the $LnFeAsO_{1-y}$ family (with Ln–Ho, Y, Dy, Tb, Gd, Sm, Nd, Pr, Ce, and La) were found to be 50.3, 46.5, 52.2, 48.5, 53.5, 55, 53, 51.3, 46.5 and 31.2 K respectively [132, 134, 135]. The onset T_c in these compounds increased with the decrease in size from the Ln atom and reached a maximum of 55 K for Sm. The crystal structure of $LnFeAsO_{1-y}$ (Ln–La, Nd) is modified compared with that of LnFeAsO. The $FeAs_4$ coordination in $LnFeAsO_{1-y}$ transforms into a regular tetrahedron with increasing oxygen deficiency accompanied by an increase in T_c, and T_c reaches a maximum when the $FeAs_4$ lattice forms a regular tetrahedron [45].

Density functional theory calculations [166] show that both oxygen vacancies and F doping act in a similar way to introduce charge carriers into the FeAs layer. But Mossbauer studies say that there are differences in the magnetic environment experienced by the Fe ions in oxygen deficient samples compared with F doped ones [167, 168]. NMR studies on $LaFeAsO_{1-y}$ ($y = 0$, 0.25, 0.4) and $NdFeAsO_{0.6}$ state that the enhancement in T_c is strongly related to the optimal local configuration of Fe and As atoms and the optimal band structure derived from the hybridization between As 4p orbital and Fe 3d orbital [105].

Wu *et al* [169] point out that annealing in high vacuum instead of applying high pressure cannot realize superconductivity in oxygen deficient $LaFeAsO_{1-y}$, while it is possible in Sr doped $La_{0.85}Sr_{0.15}FeAsO_{1-y}$ [134]. Yang *et al* [19] also reported that the oxygen deficient $SmFeAsO_{1-y}$ superconductor can be prepared only by the HP method. In order to produce enough oxygen deficiency, high pressure is essential. But there is an argument that a simple one step solid state reaction can help in preparing good quality oxygen deficient samples [170]. Like oxygen deficiency in the '1111' system, Se deficiency also plays a key role for stabilizing superconductivity in the '11' (FeSe) system [28].

Theoretical calculations proposed by Lu *et al* [171] and Zhang *et al* [172] suggested that the enhancement of DOS can be achieved either by carrier doping or by pressure. Takahashi *et al* [12] suggested that the application of external pressure can increase T_c. They reported a T_c of 43 K in a F doped LaFeAsO system under an external pressure of 4 GPa. Pressure enhancement increased the charge transfer between the insulating (LnO) layer and the conducting (FeAs) layer; in addition, the external pressure induced an anisotropic shrinkage, which is considered as the main reason for the further increase in onset T_c. Applying pressure also improves sample connectivity, a consequence of grain compaction under pressure. But the linear relationship between pressure and T_c continues until a maximum value, above which a further increase in pressure leads to a decrease in T_c. The T_c (zero) increases more slowly, which causes the broadening of the superconducting transition with an increase in pressure. The strain developed in the sample during preparation is the reason behind the broadening effect. This result is in agreement with the findings of Zocco *et al* [110]. Pressure induced superconductivity was also found in the parent compound LaFeAsO at 12 GPa with $T_c = 21$ K, and the dependence of T_c on applied pressure was similar to those of the F doped series [111].

Lu *et al* [171] studied the pressure effect on the superconducting properties of $LnFeAsO_{1-x}F_x$ ($x = 0.11$) by plotting the differential diamagnetic susceptibilities ($d\chi/dT$) against T at various pressures. (The peak of $d\chi/dT$ is manifested as the transition temperature T_c.) Pressure played a key role in pushing the low T_c superconducting phase towards the main superconducting phase. However, the studies on $CeFeAsO_{0.88}F_{0.12}$ and $LnFeAsO_{0.85}$ (Ln = Sm and Nd) systems show a negative pressure dependence of transition temperature, as shown in figure 7 [110, 130]. First-principle calculations based on density functional theory says that the origin of the negative pressure effect on T_c is due to the decrease in the electron density of states at the Fermi level. T_c increases with applied pressure only if the sample is underdoped. Therefore, the effect of pressure is more

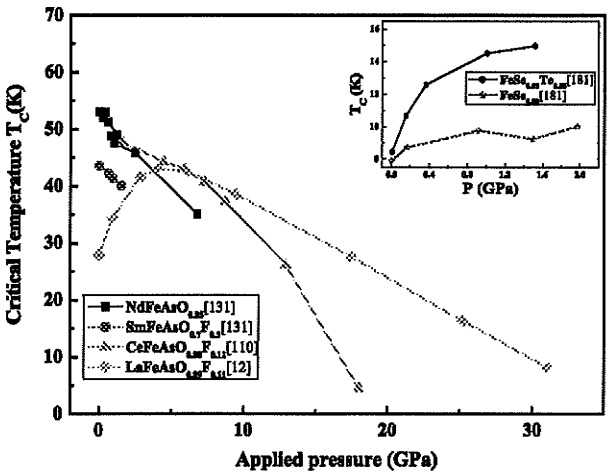

Figure 7. The effect of pressure on critical temperature in '1111'-type superconductors (the inset shows that of '11'-type).

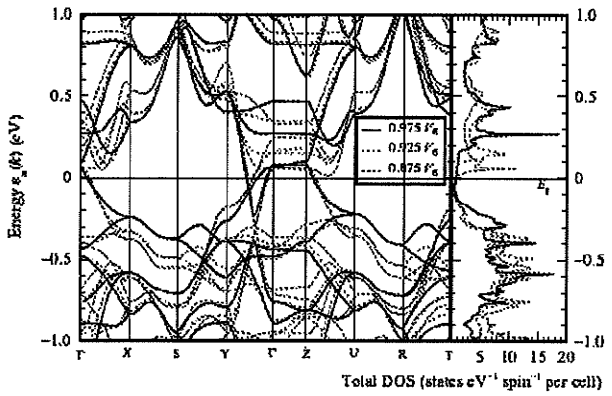

Figure 8. The effect of pressure on the band structure and DOS of the LaFeAsO system (V_0 represents the volume of LaFeAsO) [176].

complicated than simply changing the carrier concentration. The results of Lorenz *et al* [173] on $SmFeAsO_{1-x}F_x$ also agree with the previous results, i.e. pressure can either suppress or enhance T_c depending on the doping level. The pressure dependence of T_c is such that dT_c/dP can be negative or positive, the sign changes from positive to negative at the quantum critical point (QCP) [13].

Studies on $NdFeAsO_{1-x}F_x$ under pressure revealed a phase transition from the low pressure tetragonal (LPT) structure (large c-value and small a-value) to the high pressure tetragonal (HPT) structure (large a-value and small c-value). The T_c reaches its maximum before the phase transition and has a negative pressure dependence for the HPT phase. In the HPT phase, with enhanced interlayer coupling, the magnetic rare earth cation closer to the superconducting FeAs layer will break the superconducting pairs or the hybridization of the f and conduction electrons, leading to the lowering of T_c [174, 175].

The modification of crystal structure would cause a change in the electronic structure and hence a change in the transition temperature T_c. The band structure of oxypnictides also depends on the crystal structure and hence on the external pressure [176]. The effect of pressure on the band structure is shown in figure 8. The positions of the bands change under pressure, as shown in the corresponding density of states (DOS) (right panel of figure 8). The first peak above E_F is moved towards the Fermi level when pressure is applied, but the DOS from -0.1 eV to E_F is left almost unchanged by pressure. This difference suggests that pressure should induce changes in the superconducting properties.

Pressure effect studies on the FeSe-system ('11' system), to be considered as a fundamental structural unit of the more complicated Fe based superconductors, is expected to give more details of superconducting mechanisms in iron based systems [177, 178]. The pressure effect of $FeSe_x$ is larger than that of $LnFeAsO_{1-x}F_x$, as T_c reaches a maximum of 37 K at 7–9 GPa, much greater than that at ambient pressure (8 K) [16, 28, 178]. '11' systems exhibit a positive pressure coefficient, as shown in the inset of figure 7. The difference in the slope of the two plots results from the more distorted lattice for the Te doped sample under pressure, because the c-axis length of the Te doped sample is larger than that of the undoped one, which seems an indication of phonon mediated superconductivity in these compounds.

Huang *et al* [177] introduced two scenarios for the behaviour of T_c (P) in FeSe systems: (a) At low pressure the grains in the sample are tightly packed, hence showing a higher T_c. At modest pressure, the increase of DOS further enhances the superconductivity, but as the pressure continues to rise, the lattice stiffening effect reduces the T_c. (b) The $FeSe_{0.5}Te_{0.5}$ undergoes a structural transition at $P = 1.9$ GPa, which either enhances T_c or leads to a high pressure phase that favours non-superconductivity, hence giving a decreased T_c.

Superconductivity was also observed in the AFe_2As_2 (A = Ba, Sr, Ca, and Eu) type by applying external pressure, but the T_c values obtained were comparable to that found in chemically substituted samples [179, 180]. According to [181], the structural changes of the superconducting FeAs layer occurring as a function of pressure mimic those that occur as a function of chemical substitution.

5. Superconducting properties

5.1. Critical field

The upper critical field H_{c2}, and the critical current density J_c, are two important parameters to characterize superconductivity. H_{c2} is an intrinsic property of a type II superconducting material in which the resistive transition (ρ–T) width increases with increasing magnetic field, H as shown in figure 9. Usually, the H_{c2} of the sample can be measured from the resistive transition (ρ–T) analysis under different magnetic fields. According to the conventional BCS picture, H_{c2} is linear in T near T_c and saturates at the 0 K limit. This behaviour may deviate on considering the presence of impurity scattering.

The $H_{c2}(0\ \mathrm{K})$ can be calculated using the one band Werthamer–Helfand–Hohenberg (WHH) formula, $H_{c2}(0\ \mathrm{K}) = -0.693T_c[dH_{c2}/dT]_{T_c}$, where $[dH_{c2}/dT]_{T_c}$ is obtained from

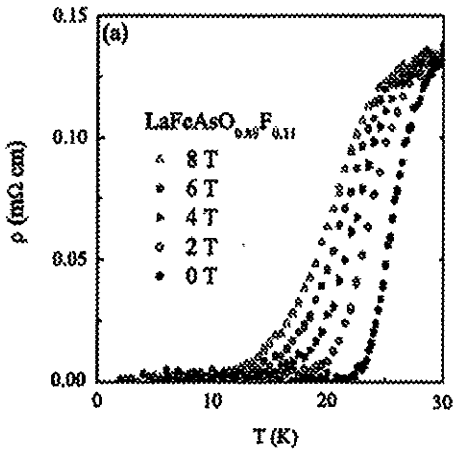

Figure 9. The temperature dependence of resistivity (ρ) at different magnetic fields (H). Reprinted figure with permission from [10]. Copyright (2008) by the American Physical Society.

the slope of the graph H_{c2} versus T at T_c. The dependence of upper critical field versus temperature for various Fe based superconductors is shown in the figure 10. Rather high values of H_{c2} are obtained for the new Fe based superconductors using the above equation and are listed in table 2, all are well above that of Nb_3Sn ($H_{c2}(0) = 30$ T for Nb_3Sn) [182]. However, these H_{c2} values are extrapolated from measurements at low magnetic field and high temperature using the one band WHH model, which is not valid for the low temperature range.

Studies of high field measurements in this superconductor reveals a two band superconductivity, that is an upward curvature of $H_{c2}(T)$, similar to MgB_2 [183, 188–191]. The two band mechanism proposed for the new superconductor suggests that the H_{c2} values can be further increased. H_{c2} can also be calculated using the Ginzburg–Landau (GL) equation [185], $H_{c2} = H_{c2}(0)(1-t^2)/(1+t^2)$, where $t = T/T_c$ is the reduced temperature. The zero temperature upper critical field determined using GL theory (56 T) was higher than that using WHH (45 T) for the $LaFeAsO_{0.9}F_{0.1-\delta}$ system [192]. The H_{c2} values obtained from the pulsed field measurements up to 55 T using a tunnel diode oscillator technique (50 T) and microwave surface impedance measurements (56 T) on the same system also agree with the GL theory [14, 193]. Based on recent reports, a very high critical field of 122 T (by WHH extrapolation) was obtained for the La based system using KF as a source of fluorine instead of LaF_3 [194].

The temperature dependence of the in-plane ($H_{c2} \parallel ab$) and out-of-plane ($H_{c2} \parallel c$) upper critical field of the new superconductor is different [20, 24, 183]. $H_{c2} \parallel c$ exhibits a significant upward curvature that is less pronounced for $H_{c2} \parallel ab$ in both single and polycrystalline studies [20, 24, 195, 196]. Thus this behaviour is an intrinsic feature of oxypnictide rather than a manifestation of vortex lattice melting or granularity, explained by the two band model [24]. The *ab initio* calculations on LaFeAs(O, F) say that superconductivity arises from two bands, a nearly 2D electron band with in-plane diffusivity, $D1$, and a more isotropic heavy hole band with smaller diffusivity, $D2$ [61]. According to the two gap

Table 2. Extrapolated values of H_{c2} using the WHH method [103, 183–187].

Type of iron pnictide compound	1111					122	11
	La	Sm	Nd	Pr	Ce	(Ba, K)Fe_2As_2	Fe(Te, Se)
Extrapolated values of H_{c2} using the WHH method (T)	36	150	204	72	107	100	87

scenario, the upward curvature of the $H_{c2}(T)$ is controlled by the ratio $\eta = D2/D1$. For $\eta \ll 1$ the upward curvature is pronounced, while for $\eta \sim 1 H_{c2}$ exhibits WHH behaviour [191]. Considering $D1^{ab} \gg D1^{c}$, for a field along the ab plane, the upward curvature of $H_{c2} \parallel ab$ becomes less pronounced than for $H_{c2} \parallel c$ [197].

The temperature dependence of H_{c2} for the '122' and '11' systems are also shown in figure 10 and are quite different from the other layered superconductors [187, 189, 198–200]. $H_{c2}(T)$ in the 122 system (hole doped (Ba, K)Fe_2As_2 [186] and electron doped Sr(Fe, Co)$_2As_2$ [201]) shows a convex shape for $H_{c2} \parallel ab$, but follows an almost linear temperature dependence down to 10 K for $H_{c2} \parallel c$. The evaluation of $H_{c2}(T)$ for $H \parallel ab$ leads to a lower $H_{c2}(0)$ (70 T) than that obtained from the extrapolation method (100 T) [186, 189]. Similar behaviour of H_{c2} has also been seen in the '11' system, in which H_{c2} in two field orientations merge together as $T \longrightarrow 0$ K at H_{c2} 47 T, less than that obtained from WHH method (85 T) [187]. The different behaviour of these systems is associated with its distinctive Fermi surface topology (3D electronic band structure) which permits orbital limiting of upper critical field at all field orientations. These results suggest that reduced dimensionality is not necessarily a prerequisite for high temperature superconductivity, in contrast to common assumptions based on the properties of the cuprates [186].

However, studies on single crystals of $NdFeAsO_{0.7}F_{0.3}$ at very high magnetic field up to 60 T, by Jaroszynski *et al* [24], show a spin dependent positive magneto-resistance for $H \parallel c$ due to the presence of some paramagnetic phase of Nd^{3+} ions. They introduce several pairing scenarios in order to explain the H_{c2} versus T curve and the best fit is obtained by considering the paramagnetic effect. The paramagnetic effect on $H_{c2}(T)$ in oxypnictides significantly reduces $H_{c2}(0)$ as compared to that based on extrapolations of $H_{c2}(T)$ near T_c down to low temperatures. The extrapolation of H_{c2} near T_c to low temperatures following the G.L. theory neglects the essential paramagnetic limitations and could overestimate the actual $H_{c2}(0)$ [195]. The extrapolated H_{c2} values are two or three times higher than the weak coupling Pauli-limited field, the field at which the free energy in the normal state becomes equal to the condensation energy of the superconductor, which may indicate a considerable enhancement of the Pauli-limited field by the strong coupling effect. The studies on an As-deficient La based system at very high magnetic field also give an insight into the onset of Pauli-limited behaviour for $H \parallel ab$ [196]. At sufficiently large magnetic field the superconductivity is destroyed by orbital and spin pair

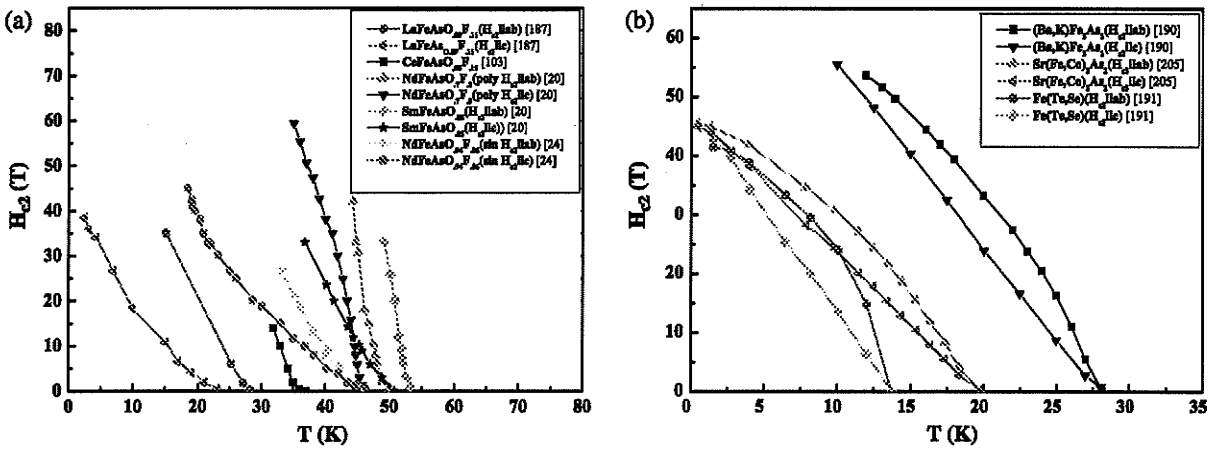

Figure 10. H_{c2} versus temperature plot for (a) '1111' type (b) '122' and '11' type iron pnictides.

breaking which leads to the flattening of $H \parallel ab$ at a lower temperature range. The suppressed upper critical field at lower temperature and higher magnetic field might also be attributed to some enhanced local exchange field acting on the superconducting charge carriers caused by an increasing alignment of localized extrinsic magnetic moments in the vicinity of As vacancies.

Recent studies on the $FeSe_{1-x}Te_x$ system show that it is necessary to include Pauli paramagnetic limiting effects (spin–paramagnetic pair breaking effect) in order to explain the temperature dependence of H_{c2} for both the field directions, in addition to orbital effects arising with different anisotropies of the Fermi velocities for the two bands [198, 199]. It is also observed that Pauli-limitation plays a larger role in this system than the other Fe based superconductors. This shows that the orbital H_{c2} is higher in this system, indicating smaller Fermi velocities and a higher effective mass than other systems.

The upper critical field of polycrystalline samples is also substantially influenced by the weak link between the grains as well as the vortex flow behaviour. Therefore, H_{c2} determination in these compounds may be complicated by the strong vortex pinning and grain disorientation distribution [183, 192]. The granular nature of the new superconductor was revealed by magnetic susceptibility measurements in these superconductors. At high temperatures, superconductivity arises due to the contribution from individual grains of the material (intragranular superconductivity) which are electrically disconnected from each other; but at low temperatures intergrain superconductivity is dominant, because the connections between the neighbouring grains become superconducting in that temperature range. Studies revealed that the vortex dynamics occurring inside the grains and that produced between the grains are different and change with external parameters such as the frequency and amplitude of the applied magnetic field [15]. These results suggest that different vortex dynamics are dominant in this new superconductor.

Thermal fluctuations of vortices also affect the H_{c2} values of oxypnictides, as in cuprate based superconductors. High T_c oxypnictides, such as Sm and Nd based systems exhibit a larger mass anisotropy and enhanced thermal fluctuations. But $LaFeAsO_{1-x}F_x$, a member of the oxypnictide family, behaves like a MgB_2 superconductor, in which the effect of thermal fluctuations of vortices is not significant. Thus the new superconductor bridges a conceptual gap between conventional superconductors and the high-T_c cuprates [20, 24, 183, 190, 202, 203]. The dissipative phenomenon, associated with the vortex motion (i.e. thermally activated flux flow and flux creep) inside the sample, limit the use of this superconductor, similar to what has been observed in YBCO. The magnetic properties using ac and dc magnetic techniques show that the new superconductor could be both linear and nonlinear. Both the flux flow (FF) and thermally activated flux flow (TAFF) are nonlinear dissipative phenomena in the absence of a dc magnetic field. But with a dc magnetic field, higher than the ac one, the field dependence of FF and TAFF resistances disappears, and generates a linear diffusion process in the magnetic field. A vortex glass phase characterized by a collective flux creep exists in LaFeAsOF oxypnictide [15, 203]. The flux creep rate with respect to field, determined using the sweep creep method proposed by Pust *et al*, is large and comparable to that in high temperature superconducting materials [204, 205].

Temperature and field dependences of the magnetization $M(T, H)$ studies on $NdFeAsO_{0.94}F_{0.06}$ reveal that the sample acts as a paramagnetic superconductor similar to $Nd_{0.85}Ce_{0.15}CuO_4$, different from both conventional superconductors and $LaFeAsO_{1-x}F_x$ oxypnictides [204]. A knee-like structure observed in the resistive transition of $NdFeAsO_{0.82}F_{0.18}$ samples [23], like in cuprate superconductors and MgB_2, suggests that a strong intrinsic pinning also occurs in iron based superconductors [206, 207]. The pinning energy of the material is 2–3 times larger than that of Bi-2212 and ten times greater than that of Bi-2223 in both low and high fields (figure 11). Compared to MgB_2 thin films its value is low at $H < 8$ T, but high at $H > 8$ T, indicating the strong pinning characteristics of $NdFeAsO_{0.82}F_{0.18}$ in high magnetic fields [208–211]. Like high temperature superconductors and MgB_2 the temperature dependence of resistivity in the broadened region of the ρ–T plot is given by $\rho(T, B) = \rho_0 \exp(-U_0/KT)$, where U_0 is the flux flow activation energy. In several works, the pinning mechanism in

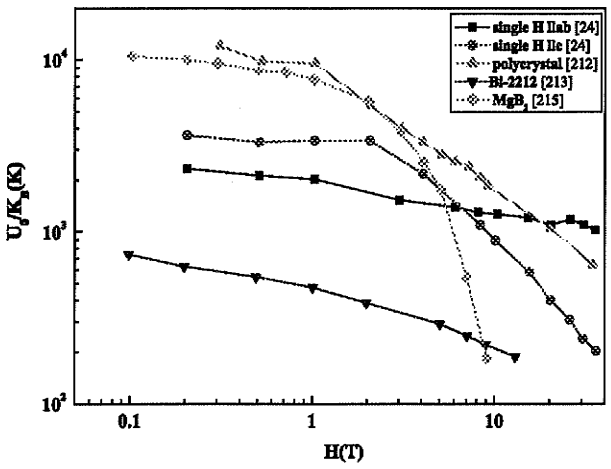

Figure 11. Magnetic field dependence of activation energy of $NdFeAsO_{0.82}F_{0.18}$ compared with Bi-2212 and MgB_2.

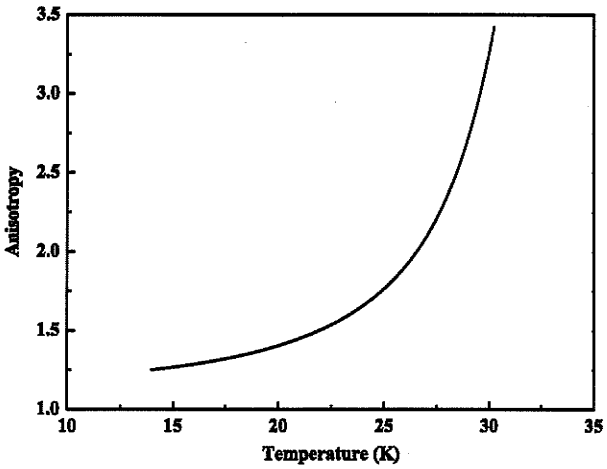

Figure 12. Temperature dependence of anisotropy in '122' systems. Reprinted figure with permission from [200]. Copyright (2008) by the American Physical Society.

this new superconductor is explained with the collective vortex pinning theory, i.e. vortex (vortex bundles) are pinned collectively by many weak pinning centres [208, 212]. Theoretical studies based on this theory revealed that this pinning mechanism is controlled by variation in the mean free path instead of variations in the critical current density [208]. Single crystal studies exhibit a conventional field dependence for $H \parallel c$ characteristic of thermally activated transport, i.e. a constant value at low fields where single vortex pinning dominates, followed by a power law decrease $U_0 \propto H^{-1.1}$ characteristic of a collective creep at higher fields. But U_0 for $H \parallel ab$ exhibits a weak power law decrease, $U_0 \propto H^{-0.17}$, in the entire field [24].

For iron oxypnictides, an increase in H_{c2} with a decrease in T_c was accomplished; this is a multiband superconducting property [194, 213]. In $CeFeAsO_{1-x}F_x$, the H_{c2} increases from 43 to 94 T when the T_c value changes from 42.5 K ($CeFeAsO_{0.8}F_{0.2}$) to 38.4 K ($CeFeAsO_{0.9}F_{0.1}$) [213]. Similar to high T_c cuprates, a doping dependence of H_{c2} is obtained for underdoped samples in the La based system, (H_{c2} = 73 T for $LaFeAsO_{0.95}F_{0.05}$ and H_{c2} = 63–65 T for $LaFeAsO_{0.89}F_{0.11}$), that is H_{c2} systematically decreases with an increase in the doping concentration (x) in the underdoped region [214, 215]. This indicates that excess F doping weakens the pairing potential, since higher H_{c2} corresponds to a stronger pairing potential. The doping dependence H_{c2} may also be understood in terms of an increase of density states and the opening of a pseudogap which increases with decreasing x-value. In addition, in underdoped samples the field induced low temperature normal state resistivity shows a positive magneto-resistance that increases with decreasing magnetic field, different from both high T_c superconductor and heavily F doped samples, in which the resistance at high field saturates to a finite value. This criterion is also satisfied in Sm based systems [16, 103]. Like the T_c of the sample, H_{c2} values can also be enhanced by the high pressure synthesis method. A higher upper critical field of 80–230 T has been exhibited by a high pressure synthesized $NdFeAsO_{0.82}F_{0.18}$ bulk sample with T_c of 51 K, greater than that of all conventional superconductors including MgB_2 [185]. An upper critical field of 37 T was reported in FeSe at ambient pressure, which was ramped up to 72 T by applying a pressure of 1.48 GPa, and 65–75 T in electron (Pt at Fe site) and hole (K at Ba site) doped '122' systems [150, 200]. The pressure effect for the enhancement of H_{c2} is remarkable in FeSe [178].

The anisotropy of iron pnictides was seen to be different for different samples. Anisotropy, H_{c2ab}/H_{c2c}, of around five was seen in $NdFeAsO_{0.82}F_{0.18}$ single crystals grown by using the flux method; this value is even below that for YBCO single crystals [23]. This is again a very important result which indicates that the anisotropy is not that strong and is very promising for applications. Comparatively moderate anisotropy, $\approx$3.5 at $T_c \approx$ 30 K, was also reported in '122' systems, dropping to 1.2 at 14 K, as shown in figure 12 [200, 216]. The anisotropy of low critical field (H_{c1}) is observed to be temperature dependent, i.e. H_{c1} slightly decreases with decreasing temperature, which is evidence for multiband superconductivity [217]. The irreversibility field (H_{irr}) is another important factor which limits the application of superconductors. Relatively higher irreversibility field is obtained for the new Fe based superconductor than for MgB_2 superconductors [23]. It is now well established that the intra and inter band scattering mechanisms present in oxypnictides control H_{c2} and H_{irr} [218]. The high values of H_{c2} and H_{irr} make the new superconductor promising for magnetic field applications.

5.2. *Critical current density*

From the application point of view, the critical current density J_c is another important parameter to be discussed for the new superconductor. It is sample dependent and controlled by the flux pinning properties. Actually, in polycrystalline samples, there exists two distinct scales of shielding current densities—local and global current densities, due to the granularity of the sample. The current flow within the grains is called the intragrain critical current density (J_{clocal}) and current

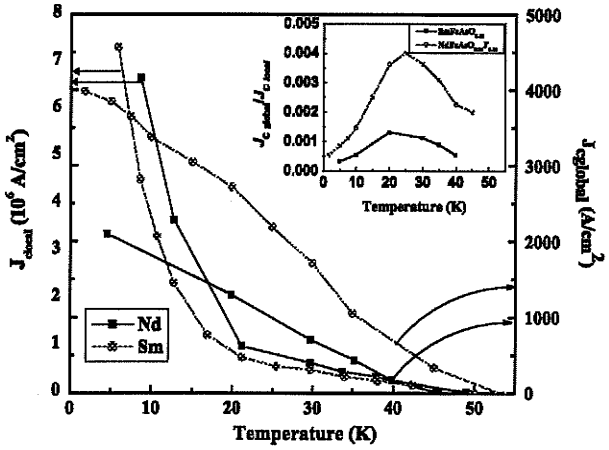

Figure 13. Temperature dependence of global and local critical current densities (J_c) in Fe based superconductors [220].

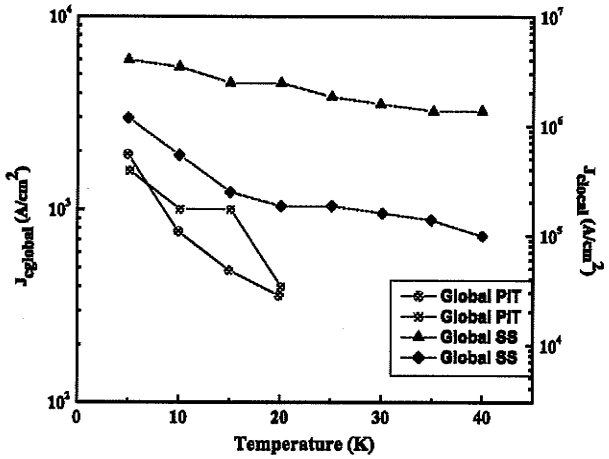

Figure 14. Dependence of critical current densities on different preparation methods [225].

throughout the sample is called the intergrain critical current density ($J_{cglobal}$). J_{clocal} is dominated by vortex pinning while $J_{cglobal}$ is dominated by connections across grain boundaries, which are not superconducting. Magneto-optical imaging (MO) and remanent magnetic field analysis on Nd and Sm samples reveal these dependencies [219]. $J_{cglobal}$ also depends on the voids present in the sample.

Critical current density of the sample can be calculated using the Bean model from the hysteresis loop, $J_c = \frac{20\Delta m}{a(1-\frac{a}{3b})}$, where Δm is the height of the magnetization loop, and a and b are the dimensions of the sample perpendicular to the magnetic field. But J_c within the grains can be calculated using the equation $J_c = 3\Delta m/\langle R\rangle$, where $\langle R\rangle$ is the average grain size. A relatively large J_c is observed in the Nd and Sm samples, of the order of 10^4 A cm^{-2} at 5 K, which is better than that in the polycrystalline cuprates [220, 221]. Electrical transport studies on oxygen deficient fluorine free $NdFeAsO_{1-x}$ also show that there are well connected current paths through the whole sample [222]. But these results are in strong contrast to the almost zero bulk current observed in the $LaFeAsO_{0.89}F_{0.11}$ sample [223]. A large current carrying ability is also reported in the $Ba_{0.6}K_{0.4}Fe_2As_2$ system at 9 T ($J_c > 1 \times 10^6$ A cm^{-2} at 5 K) [224].

Studies show that $J_{cglobal}/J_{clocal}$ slightly increases with increasing temperature up to a particular temperature (inset of figure 13) and decreases rapidly at higher temperature due to thermal fluctuations of vortices. J_{clocal} shows a linear temperature dependence near T_c, this dependence and the very high J_{clocal} are indications of strong intragrain vortex pinning. The temperature dependence of J_{clocal} is smaller than that of $J_{cglobal}$. The influence of grain connectivity on $J_{cglobal}$ is responsible for its large temperature and magnetic field dependence. The temperature dependence of $J_{cglobal}$ near T_c also suggests a superconducting–normal–superconducting proximity coupled Josephson junction, which has been also observed in cuprate superconductors. So the intergranular current transport in the sample is limited by the proximity coupled conductive As–Fe phase and/or by the intrinsic weak

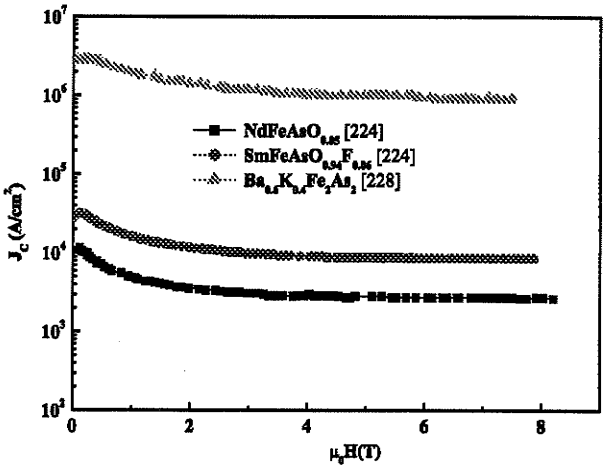

Figure 15. Magnetic field dependence of critical current densities (J_c) in Fe based superconductors.

coupling [220]. $J_{cglobal}$ is also size dependent because the field of penetration should be proportional to the $J_{cglobal} \times$ (sample size). However, the J_{clocal} is size independent, nevertheless it depends on the preparation methods, i.e. its value is found to be larger for PIT (powder-in-tube) wires than bulk ones (figure 14). However, $J_{cglobal}$ is more or less identical for both types [225].

The field dependence of the critical current density is another limiting factor for its magnetic field applications (figure 15). According to collective vortex pinning theory, the critical current density is field independent when the applied magnetic field is lower than the crossover field B_c. Below B_c the sample is in the single vortex pinning regime. Studies show some small deviations from the above statement due to the transition from the single vortex pinning regime to the small-bundle-pinning regime. This is in agreement with collective vortex pinning present in the new superconductor [208]. The temperature dependence of J_c also

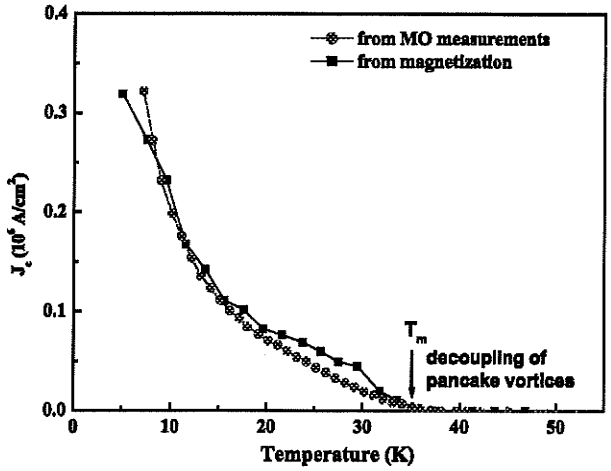

Figure 16. Critical current density versus temperature in $NdFeAsO_{0.9}F_{0.1}$ [226].

shows a sharp crossover in the pinning mechanism, i.e. a crossover from 3D Josephson coupled pancake vortices to 2D pancakes, and at that temperature (T_m) J_c vanishes, as seen in figure 16. The order of magnitude and overall temperature dependence of J_c is quite similar to that observed in BSCCO-2212 [226, 227].

Magneto-optical imaging gives a direct observation of the local magnetic flux structure of the sample. Strong flux fields in the flux penetrated region revealed from the MO images is an indication of a local circulating current with a higher current density [219]. But the impurity phases present in the Sm and Nd samples lower the J_c. In weakly coupled polycrystals the weakening occurs either at grain boundaries or at the impurity phases. But flux penetration is expected to occur locally at lower fields than into the grains. Combined low temperature laser scanning microscopy and scanning electron microscopy on Sm based samples [228] revealed the presence of both the wetting Fe–As phase, which is a normal-metal wetting-phase surrounding the superconducting grains producing a dense array of superconducting–normal–superconducting contacts, and cracks at grain boundaries, which interrupt the grain to grain supercurrent path. In the Nd based sample ($NdFeAsO_{0.82}F_{0.18}$) the supercurrent density drops only by a factor of 2–6 for $T < 30$ K when the field changes from 1 T to 9 T, significantly slower than that of MgB_2 and high T_c cuprate superconductors [185]. Its superior J_c–field performance is promising for the use of oxypnictide superconductors in high field applications. But direct current transport studies (E–J at different magnetic field) on Sm samples [228] show that the transport J_c switched off with the application of an external field (>5 T) due to the presence of cracks and a wetting Fe–As phase at the grain boundaries produced by thermal stress during the sample preparation. Therefore, synthesis methods have to be optimized in order to get better quality samples with high transport current. Still, their high H_{c2} and weak J_c—field dependence make them a powerful competitor for high field applications.

6. Thermal properties

Specific heat measurement is one of the tools to measure DOS at the Fermi level. The measurements were performed using thermal relaxation techniques. Specific heat studies were conducted for $LaFeAsO_{1-x}F_x$ by many groups [10, 77, 229–231]. A clear specific heat jump was observed at about 150 K for LaFeAsO which was accompanied by anomalies in resistivity, Hall coefficient, and Seebeck coefficient [77, 229]. These anomalies are suspected to be due to structural distortion or a SDW transition or both. McGuire *et al* reported the heat capacity measurement of LaFeAsO, where the subtracted data of specific heats ($C_p - C_{pbackground}$) versus temperature exhibited two peaks, one associated with a structural transition at 155 K and the other with a magnetic transition at 143 K, suggesting that the anomalies are not due to a single transition smeared by inhomogeneities. The phase transition was proposed to be either second order or weakly first order, with a total change in entropy of 1.7 mJ mol^{-1} K^{-1}. No specific heat anomaly was detected near T_c [230]. All these point towards the low superfluid density of $LaFeAsO_{1-x}F_x$.

A specific heat study of $SmFeAsO_{1-x}F_x$ ($0 \leqslant x \leqslant 0.2$) was reported by Ding *et al* [231]. The undoped sample showed an anomaly near 130 K while the doped superconducting sample exhibited an anomaly near T_c. The specific heat value largely exceeded the Dulong–Petit value and strongly depended on F doping. Later, Tropeano *et al* reported on a similar study [17], which summarized that the electron–phonon coupling strongly characterizes the thermal properties, giving an idea of electronic ground states. The specific heat saturated on the Dulong–Petit value in contradiction to the former study.

A low temperature specific heat measurement performed on $Ba_{0.6}K_{0.4}Fe_2As_2$ and $SmFeAsO_{0.9}F_{0.1}$ samples by Mu *et al* [232] showed an anomaly with a higher value of $(\Delta C/T)$ at T_c for $Ba_{0.6}K_{0.4}Fe_2As_2$ than for $SmFeAsO_{0.9}F_{0.1}$. Specific heat measurements on $LaFeAsO_{0.9}F_{0.1-\delta}$ revealed a nonlinear magnetic field dependence of the specific heat coefficient in the low temperature limit, as predicted for a nodal superconductor [230]. The Debye temperature θ_D was determined (almost 170 K for FeAs superconductor) and used in the Macmillan equation, it suggested that a simple electron model cannot explain the superconducting mechanism of iron oxypnictide. The specific heat coefficient of $Ba_{0.6}K_{0.4}Fe_2As_2$ was found to be weakly dependent on temperature while showing a linear dependence on magnetic field in contradiction to LnFeAsO samples. The report [232] makes a clear distinction between the properties of the two groups which originate from complex Fermi surface structures in them. Specific heat studies on heavily hole doped KFe_2As_2 show a clear jump near T_c (3.5 K) indicating the bulk nature of superconductivity [233]. The finite specific heat (C_{QP}/T) values, even at the lowest measurement temperature, also suggest a quasi particle excitation at low energy. These results lead to a multi-gap nodal superconducting scenario which is contradictory to the thermal transport studies in Co-doped $BaFe_2As_2$, which prefer a fully gapped sign reversing s-wave superconductivity. Heat capacity measurements on

$LnFeAsO_{1-x}F_x$ (Ln = Sm, Nd, La) and LiFeAs by Baker *et al* [234] displayed λ anomalies at each Neel temperature, supporting the ordering of rare earth moments [104]. $LaFeAsO_{0.9}F_{0.1}$ and LiFeAs exhibited distinct anomalies at T_c. In short, almost all the results matched well with the previous reports.

Thermoelectric power (TEP) measurements of iron pnictides can help in better understanding its superconducting and transport properties in the normal state. It can give clues to the entropy flux during charge transport, the change of electronic band structure at the Fermi level, phase transitions and electron–phonon coupling. Iron arsenides are seen to have thermoelectric power even larger than 1 mW m^{-1} K^{-2} around 80–100 K. Thus they are proposed to be good candidates for refrigeration applications at liquid nitrogen temperatures [235]. The values of TEP over the measured temperature range are negative, suggesting electron-like charge carriers, which supports the results from the Hall-effect studies [10, 14, 192]. The anomalous dependence of TEP on temperature and pressure is attributed to resonant phonon scattering between electron and hole pockets, an outcome of Fermi surface nesting. TEP measurements on parent compounds have shown signs of SDW order [236]. In short, studies on TEP, thermal conductivities and specific heat capacities of iron based compounds have given much insight into their diverse superconducting mechanisms.

7. Comparison of iron based superconductors with other high T_c superconductors

Iron based superconductors are the first non-cuprate materials exhibiting superconductivity at relatively high temperatures upon electron or hole doping of non-superconducting antiferromagnetic parent compounds. The two-dimensional electronic structure [10, 61], the presence of a superconducting dome in the electronic phase diagram, where the T_c is controlled by a systematic aliovalent ion doping into the insulating block layers [14], and the anomaly in the transport property in the under doped region [15, 66], make iron based superconductors similar to cuprates from the first investigations.

The tetragonal-to-orthorhombic phase transition study in multiband FeAs superconductors reported by Ricci *et al* hints to a similarity with cuprates in the emergence of the superconducting phase as super stripes and lattice charge instability which can be varied by external fields [237]. Density functional theory calculations in LaFeAsO reveal that the antiferromagnetic exchange interaction and frustrated ground state have many common magnetic properties with the undoped parent compound of high T_c cuprates [47]. Cuprates and iron based superconductors are similar in the occurrence of unusual normal state properties which are outside the framework of Fermi liquid theory [238]. Though they share some similarities, there are enough properties which make iron pnictides different. The parent materials in cuprates are Mott insulators where a single electron is localized on the copper site, while those of iron oxypnictides are antiferromagnetically ordered metallic itinerant electron systems. For the cuprates all the spin structures in the *ab* plane are simple collinear antiferromagnets, while in iron based superconductors iron spins order only when the crystal distorts, with the spin parallel in one direction and antiparallel in the other [102]. In both classes of materials, high temperature superconductivity arises from strong attractive interactions between carriers generated by the local structural [239, 240] and chemical changes associated with valency changes, Cu^{2+} to Cu^{3+} in the cuprates and Fe^{2+} to Fe^{+} in the pnictides, and from the accompanying changes in the local spin order [241]. At low temperatures, both the groups exhibit spectral weight suppression, the big difference being that the suppression in iron based superconductors is doping dependent. The correlation found between the lattice and the critical temperature for cuprates matches well with iron based superconductors [50]. Both cuprates and iron oxypnictides show lattice contraction and T_c enhancement with fluorine doping [241, 242]. But the superconductivity induced in FeAs layers is insensitive to randomness unlike that in the CuO_4 planes of high T_c cuprates [237, 243–245]. Moreover, the pressure effect on T_c enhancement in iron oxypnictides is more prominent than in the cuprates, since the arsenic ion has a greater electronic polarizability owing to the covalency of the FeAs bond, and hence is more compressible than the O^{2-} ion [12].

Several groups reported on the presence and absence of the superconducting gap in iron pnictides. The existence of nodes in the superconducting gap is supported by the in-plane coherence length, temperature dependent Hall coefficient, a vanishingly small jump at T_c in the electronic specific heat and its behaviour in magnetic field, as in high T_c cuprates [192, 230, 246, 247]. Microwave penetration depth measurements on $PrFeAsO_{1-y}$ suggest that the order parameter symmetry of iron oxypnictide superconductors is fully gapped, in contrast to the cuprate superconductors [248]. Moreover, studies on $SmFeAsO_{0.85}F_{0.15}$ revealed a superconducting gap whose nature is more consistent with a BCS prediction and incompatible with theoretical models designed for HTS [249]. The presence of a pseudogap has also been argued in $LaFeAsO_{1-x}F_x$ and $SmFeAsO_{1-x}F_x$ using several neutron magnetic resonance and angle integrated photoemission spectroscopy studies. These experiments suggest a pseudogap of 9–46 k_BT_c, very similar to the 10–40 k_BT_c pseudogap scale observed in cuprate superconductors [112].

Iron based superconductors have very high upper critical fields and exhibit multiband features along with an unconventional pairing symmetry similar to cuprates [23, 183, 192, 212, 250]. But the symmetry of the order parameter in iron based superconductors is suggested as s-wave by several groups [251, 252], while it is d-wave in cuprates. $d_{x^2-y^2}$ wave pairing was also suggested for iron pnictides [94, 253]. An extended s-wave symmetry with sign reversal of the order parameter is the widely accepted one for iron pnictides [91, 166, 251]. Reports on vortex dynamics suggested vortex properties similar to those of cuprates [208, 212, 224, 226, 254]. The observation of local lattice instabilities and the complex Fermi surface topology, pointing towards multiband superconductivity, are analogous to MgB_2 [74, 255]. Some features of iron pnictides are

closer to MgB_2 while the majority are more suited to cuprates, making it a bridge between the two [237].

8. Summary

In 2008 almost all journals were flooded with articles having tantalizing titles such as 'strike iron while it is hot ..., arsenic heats up iron ..., back to iron age ...'. This review is an attempt to give a compendium on all the research that has already been done on iron pnictides within the short span of two years. The structural properties and different categories of iron based superconductors have been discussed. A summary of synthesis methods shows the necessity of an inert atmosphere, high temperature and high pressure for the preparation of high quality samples. This infers the necessity to optimize the synthesis methods so as to improve the existing status of the superconducting properties.

The effects of chemical doping and external pressure is also discussed in detail. It seems that a substantial portion of the periodic table has been tried in iron pnictides and most of them have turned out to be successful. This indicates the possibility of discovering many new compounds having layered structures and much better superconducting properties. The reports on superconducting properties such as T_c, J_c and H_{c2} of almost all iron pnictides have been summarized, and indicate that iron pnictides are promising candidates for magnetic applications. As far as technological applications are concerned, a systematic effort is needed in the fabrication of wires and tapes with the desired geometry and properties.

Being an emerging superconductor, iron pnictides are explained from different perspectives. The review also gives glimpses at the contradictory proclamations made on the superconducting mechanism behind the material. Obviously, there exists a tug of war on the topic 'whether the material is similar to or different from cuprates' [91, 95, 96, 256–258]. It is observed that iron pnictides display properties between the conventional superconductors and the high temperature ones. So the theoretical predictions and justifications for the unanswered superconducting mechanism may be cleared up given time.

Acknowledgments

J B Anooja and P M Aswathy acknowledge the Kerala State Council for Science, Technology and Environment (KSCSTE), Kerala, India and P M Sarun acknowledges the Council of Scientific and Industrial Research, India, for their Research Fellowships.

References

[1] Bednorz J G and Muller K A 1986 *Z. Phys.* B **64** 189
[2] Nagamatsu J, Nakagawa N, Muranaka T, Zenitani Y and Akimitsu J 2001 *Nature* **410** 63
[3] Kamihara Y, Watanabe T, Hirano M and Hosono H 2008 *J. Am. Chem. Soc.* **130** 3296
[4] Kamihara Y, Hiramatsu H, Hirano M, Kawamura R, Yanagi H, Kamiya T and Hosono H 2006 *J. Am. Chem. Soc.* **128** 10012
[5] Gao Z, Wang L, Qi Y, Wang D, Zhang X and Ma Y 2008 *Supercond. Sci. Technol.* **21** 105024
[6] Gao Z, Wang L, Qi Y, Wang D, Zhang X, Ma Y, Yang H and Wen H 2008 *Supercond. Sci. Technol.* **21** 112001
[7] Hiramatsu H, Katase T, Kamiya T, Hirano M and Hosono H 2008 *Appl. Phys. Express* **1** 101702
[8] Choi E, Jung S, Lee N H, Kwon Y, Kang W N, Kim D H, Jung M, Lee S and Sund L 2009 *Appl. Phys. Express* **2** 083004
[9] Chen Y L, Cui Y J, Yang Y, Zhang Y, Wang L, Cheng C H, Sorrell C and Zhao Y 2008 *Supercond. Sci. Technol.* **21** 115014
[10] Sefat A S, Mcguire M A, Sales B C, Jin R, Howe J Y and Mandrus D 2008 *Phys. Rev.* B **77** 174503
[11] Shekhar C, Singh S, Siwach P K, Singh H K and Srivastava O N 2008 *Supercond. Sci. Technol.* **22** 015005
[12] Takahashi H, Igawa K, Arii K, Kamihara Y, Hirano M and Hosono H 2008 *Nature* **453** 376
[13] Takabayashi Y, Mcdonald M T, Papanikolaou D, Margadonna S, Wu G, Liu R H, Chen X H and Prassides K 2008 *J. Am. Chem. Soc.* **130** 9242
[14] Chen G F *et al* 2008 *Phys. Rev. Lett.* **101** 057007
[15] Polichetti M, Adesso M G, Zola D, Luo J, Chen G F, Li Z, Wang N L, Noce C and Pace S 2008 *Phys. Rev.* B **78** 224523
[16] Margadonna S, Takabayashi Y, Ohishi Y, Mizuguchi Y, Takano Y, Kagayama T, Nakagawa T, Takata M and Prassides K 2009 *Phys. Rev.* B **80** 064506
[17] Tropeano M, Martinelli A, Palenzona A, Bellingeri E, Dagliano E G, Nguyen T D, Affronte M and Putti M 2008 *Phys. Rev.* B **78** 094518
[18] Lu W *et al* 2008 *Solid State Commun.* **148** 168
[19] Yang J *et al* 2009 *Supercond. Sci. Technol.* **22** 025004
[20] Jaroszynski J *et al* 2008 *Phys. Rev.* B **78** 064511
[21] Bos J G, Penny G B S, Rodgers J A, Sokolov D A, Huxley A D and Attfield J P 2008 *Chem. Commun.* **31** 3634
[22] Kursumovic A, Durrell J H, Chen S K and Driscoll J L M 2010 *Supercond. Sci. Technol.* **23** 025022
[23] Jia Y, Cheng P, Fang L, Luo H, Yang H, Ren C, Shan L, Gu C and Wen H H 2008 *Appl. Phys. Lett.* **93** 032503
[24] Jaroszynski J *et al* 2008 *Phys. Rev.* B **78** 174523
[25] Rotter M, Tegel M and Johrendt D 2008 *Phys. Rev. Lett.* **101** 107006
[26] Sasmal K, Lv B, Lorenz B, Guloy A M, Chen F, Xue Y and Chu C 2008 *Phys. Rev. Lett.* **101** 107007
[27] Wang X C, Liu Q Q, Lv Y X, Gao W B, Yang L X, Yu R C, Li F Y and Jin C Q 2008 *Solid State Commun.* **148** 538
[28] Hsu F *et al* 2008 *Proc. Natl Acad. Sci.* **105** 14262
[29] Zhang X, Wang L, Qi Y, Wang D, Gao Z, Zhang Z and Ma Y 2010 *Physica* C **470** 104
[30] Backen E, Haindl S, Niemeier T, Huhne R, Freudenberg T, Werner J, Behr G, Schultz L and Holzapfel B 2008 *Supercond. Sci. Technol.* **21** 122001
[31] Kidszun M, Haindl S, Reich E, Hanisch J, Iida K, Schultz L and Holzapfel B 2010 *Supercond. Sci. Technol.* **23** 022002
[32] Han Y, Li W Y, Cao L X, Zhang S, Xu B and Zhao B R 2009 *J. Phys.: Condens. Matter* **21** 235702
[33] Imai Y, Akiike T, Hanawa M, Tsukada I, Ichinose A, Maeda A, Hikage T, Kawaguchi T and Ikuta H 2010 *Appl. Phys. Express* **3** 043102
[34] Ma F and Lu Z Y 2008 *Phys. Rev.* B **78** 033111
[35] Nomura T, Kim S W, Kamihara Y, Hirano M, Sushko P V, Kato K, Takata M, Shluger A L and Hosono H 2008 *Supercond. Sci. Technol.* **21** 125028
[36] Leblanc J P F and Nicol E J 2008 *Phys. Rev.* B **78** 094513
[37] Fratini M *et al* 2008 *Supercond. Sci. Technol.* **21** 092002

[38] Margadonna S, Takabayashi Y, Mcdonald M T, Brunei M, Wu G, Liu R H, Chen X H and Prassides K 2009 *Phys. Rev.* B **79** 014503
[39] Zhang C J, Oyanagi H, Sun Z H, Kamihara Y and Hosono H 2008 *Phys. Rev.* B **78** 214513
[40] Tyson T A, Wu T, Woicik J, Ravel B, Ignatov A, Zhang C L, Qin Z, Zhou T and Cheong S W 2009 arXiv:0903.3992v1
[41] Iadecola A, Agrestini S, Filippi M, Simonelli L, Fratini M, Joseph B, Mahajan D and Saini N L 2009 *Europhys. Lett.* **87** 26005
[42] Kurmaev E Z, McLeod J A, Skorikov N A, Finkelstein L D, Moewes A, Izyumov Y A and Clarke S 2009 *J. Phys.: Condens. Matter* **21** 345701
[43] Zhao J *et al* 2008 *Nature Mater.* **7** 953
[44] Shirage P M, Miyazawa K, Kito H, Eisaki H and Iyo A 2008 *Phys. Rev.* B **78** 172503
[45] Lee C, Iyo A, Eisaki H, Kito H, Fernandezdiaz M T, Ito T, Kihou K, Matsuhata H, Braden M and Yamada K 2008 *J. Phys. Soc. Japan* **77** 083704
[46] Si Q and Abrahams E 2008 *Phys. Rev. Lett.* **101** 076401
[47] Yildirim T 2008 *Phys. Rev. Lett.* **101** 057010
[48] Rotter M, Tegel M, Johrendt D, Schellenberg I, Hermes W and Pottgen R 2008 *Phys. Rev.* B **78** 020503
[49] Pitcher M J, Parker D R, Adamson P, Herkelrath S J C, Boothroyd A T and Clarke S J 2008 *Chem. Commun.* 5918
[50] Huber F, Roeser H P and Schoenermark M V 2008 *J. Phys. Soc. Japan* **77** 142
[51] Tapp J H, Tang Z, Lv B, Sasmal K, Lorenz B, Chu P C W and Guloy A M 2008 *Phys. Rev.* B **78** 060505
[52] Pitcher M J, Parker D R, Adamson P, Herkelrath S J C, Boothroyd A T, Ibberson R M, Brunelli M and Clarke S J 2008 *Chem. Commun.* **45** 5918
[53] Matsuishi S, Inoue Y, Nomura T, Yanagi H, Hirano M and Hosono H 2008 *J. Am. Chem. Soc.* **130** 14428
[54] Han F, Zhu X Y, Mu G, Cheng P and Wen H H 2008 *Phys. Rev.* B **78** 180503
[55] Tegel M, Johansson S, Weiss V, Schellenberg I, Hermes W, Poettgen R and Johrendt D 2008 *Europhys. Lett.* **84** 67007
[56] Zhu X Y, Han F, Cheng P, Mu G, Shen B and Wen H H 2009 *Europhys. Lett.* **85** 17011
[57] Sato S, Ogino H, Kawaguchi N, Katsura Y, Kishio K, Shimoyama J, Kotegawa H and Tou H 2010 *Supercond. Sci. Technol.* **23** 045001
[58] Ogino H, Matsumura Y, Katsura Y, Ushiyama K, Horii S, Kishio K and Shimoyama J 2009 *Supercond. Sci. Technol.* **22** 075008
[59] Chen G F, Xia T, Yang H X, Li J Q, Zheng P, Luo J L and Lwang N 2009 *Supercond. Sci. Technol.* **22** 072001
[60] Zhu X, Han F, Mu G, Cheng P, Shen B, Zeng B and Wen H H 2009 *Phys. Rev.* B **79** 220512
[61] Singh D J and Du M H 2008 *Phys. Rev. Lett.* **100** 237003
[62] Ishibashi S, Terakura K and Hosono H 2008 *J. Phys. Soc. Japan* **77** 053709
[63] Lebègue S 2008 *Phys. Rev.* B **75** 035110
[64] Raghu S, Qi X, Liu C, Scalapino D J and Zhang S 2008 *Phys. Rev.* B **77** 220503
[65] Mechelen J L M V, Marel D V D, Grimaldi C, Kuzmenko A B, Armitage N P, Reyren N, Hagemann H and Mazin I I 2008 *Phys. Rev. Lett.* **100** 226403
[66] Cruz C D L *et al* 2008 *Nature* **453** 899
[67] Huang Q, Qiu Y, Bao W, Green M A, Lynn J W, Gasparovic Y C, Wu T, Wu G and Chen X H 2008 *Phys. Rev. Lett.* **101** 257003
[68] Coldea A I, Fletcher J D, Carrington A, Analytis J G, Bangura A F, Chu J H, Erickson A S, Fisher I R, Hussey N E and McDonald R D 2008 *Phys. Rev. Lett.* **101** 216402
[69] Sugawara H, Settai R, Doi Y, Muranaka H, Katayama K, Yamagami H and Onuki Y 2008 *J. Phys. Soc. Japan* **77** 113711
[70] Sebastian S, Gillett J, Harrison N, Lau P, Singh D, Mielke C and Lonzarich G 2008 *J. Phys.: Condens. Matter* **20** 422203
[71] Zabolotnyy V *et al* 2009 *Nature* **457** 569
[72] Lu D *et al* 2008 *Nature* **455** 81
[73] Ding H *et al* 2008 *Europhys. Lett.* **83** 47001
[74] Liu C *et al* 2008 *Phys. Rev. Lett.* **101** 177005
[75] Kondo T *et al* 2008 *Phys. Rev. Lett.* **101** 147003
[76] Morinari T, Nakamura H, Machida M and Tohyama T 2009 *J. Phys. Soc. Japan* **78** 114702
[77] Dong J *et al* 2008 *Europhys. Lett.* **83** 27006
[78] Singh D J 2008 *Phys. Rev.* B **78** 094511
[79] Yi M *et al* 2009 *Phys. Rev.* B **80** 024515
[80] Samuely P, Pribulov Z, Szab P, Prist G, Budko S L and Canfield P C 2009 *Physica* C **469** 507
[81] Zhao L *et al* 2008 *Chin. Phys. Lett.* **25** 4402
[82] Evtushinsky D V *et al* 2009 *Phys. Rev.* B **79** 054517
[83] Nakayama K *et al* 2009 *Europhys. Lett.* **85** 67002
[84] Wray L *et al* 2008 *Phys. Rev.* B **78** 184508
[85] Terashima K *et al* 2009 *Proc. Natl Acad. Sci. USA* **106** 7330
[86] Mukuda H *et al* 2009 *J. Phys. Soc. Japan* **78** 084717
[87] Arita R and Ikeda H 2009 *J. Phys. Soc. Japan* **78** 113707
[88] Malaeb W *et al* 2009 *J. Phys. Soc. Japan* **78** 123706
[89] Xu G 2008 *Europhys. Lett.* **84** 67015
[90] Liu C 2009 *Phys. Rev. Lett.* **102** 167004
[91] Mazin I I and Schmalian J 2009 *Physica* C **469** 614
[92] Fang C, Yao H, Tsai W F, Hu J and Kivelson S A 2008 *Phys. Rev.* B **77** 224509
[93] Xu C, Muller M and Sachdev S 2008 *Phys. Rev.* B **78** 020501
[94] Kuroki K, Onari S, Arita R, Usui H, Tanaka Y, Kontani H and Aoki H 2008 *Phys. Rev. Lett.* **101** 087004
[95] Graser S, Maier T A, Hirschfeld P J and Scalapino D J 2009 *New J. Phys.* **11** 025016
[96] Wang F, Zhai H, Ran Y, Vishwanath A and Lee D 2009 *Phys. Rev. Lett.* **102** 047005
[97] Yao Z J, Li J X and Wang Z D 2009 *New J. Phys.* **11** 025009
[98] Sknepnek R 2009 *Phys. Rev.* B **79** 054511
[99] Nakamura K, Arita R and Imada M 2008 *J. Phys. Soc. Japan* **77** 093711
[100] Anisimov V I, Korotin D M, Korotin M A, Kozhevnikov A V, Kunes J, Shorikov A O, Skornyakov S L and Streltsov S V 2009 *J. Phys.: Condens. Matter* **21** 075602
[101] Yildirim T 2009 *Phys. Rev. Lett.* **102** 037003
[102] Chen Y, Lynn J W, Li J, Li G, Chen G F, Luo J L, Wang N L, Dai P, Cruz C D and Mook H A 2008 *Phys. Rev.* B **78** 064515
[103] Chen G F, Li Z, Wu D, Li G, Hu W Z, Dong J, Zheng P, Luo J L and Wang N L 2008 *Phys. Rev. Lett.* **100** 247002
[104] Pourovskii L, Vildosola V, Biermann S and Georges A 2008 *Europhys. Lett.* **84** 37006
[105] Mukuda H *et al* 2008 *J. Phys. Soc. Japan* **77** 093704
[106] Jishi R A and Alyahyaei H M 2009 *New J. Phys.* **11** 083030
[107] Nakai Y, Ishida K, Kamihara Y, Hirano M and Hosono H 2008 *J. Phys. Soc. Japan* **77** 073701
[108] Luetkens H *et al* 2009 *Nature Mater.* **8** 305
[109] Ren Z A and Zhao Z X 2009 *Adv. Mater.* **21** 4584
[110] Zocco D A *et al* 2008 *Physica* C **468** 2229
[111] Okada H, Igawa K, Takahashi H, Kamihara Y, Hirano M, Hosono H, Matsubayashi K and Uwatoko Y 2008 *J. Phys. Soc. Japan* **77** 113712
[112] Ou W *et al* 2008 *Solid State Commun.* **148** 504
[113] Chu C *et al* 2008 *J. Phys. Soc. Japan* **77** 72
[114] Chen G F, Li Z, Wu D, Dong J, Li G, Hu W Z, Zheng P, Luo J L and Wang N L 2008 *Chin. Phys. Lett.* **25** 2235
[115] Cheng P *et al* 2008 *Sci. China* G **51** 719

[116] Chen X H, Wu T, Wu G, Liu R H, Chen H and Fang D F 2008 *Nature* **453** 761
[117] Li L, Li Y, Ren Z, Luo Y, Lin X, He M, Tao Q, Zhu Z, Cao G and Xu Z 2008 *Phys. Rev.* B **78** 132506
[118] Wei Z, Li H O, Hong W L, Lv Z M, Wu H Y, Guo X F and Ruan K Q 2008 *J. Supercond. Novel Magn.* **21** 213
[119] Yi W *et al* 2008 *Supercond. Sci. Technol.* **21** 125022
[120] Yang J L, Ren W J, Li D, Hu W J, Li B and Zhang Z D 2008 *Supercond. Sci. Technol.* **23** 025003
[121] Che R C, Wang L, Chen Z, Ma C, Liang C Y, Lu J B, Shi H L, Yang H X and Li J Q 2008 *Europhys. Lett.* **83** 66005
[122] Wen H H, Mu G, Fang L, Yang H and Zhu X 2008 *Europhys. Lett.* **82** 17009
[123] Wu G, Chen H, Wu T, Xie Y L, Yan Y J, Liu R H, Wang X F, Ying J J and Wu X H C 2008 *J. Phys.: Condens. Matter* **20** 422201
[124] Chen H *et al* 2009 *Europhys. Lett.* **85** 17006
[125] Rotter M, Pangerl M, Tegel M and Johrendt D 2008 *Angew. Chem. Int. Edn* **47** 7949
[126] Daghero D, Tortello M, Gonnelli R S, Stepanov V A, Zhigadlo N D and Karpinski J 2009 *Phys. Rev.* B **80** 060502
[127] Chong S V, Mochiji T and Kadowaki K 2009 *J. Phys.: Conf. Ser.* **150** 052036
[128] Dmitriev V M, Kostyleva I E, Khlybov E P, Zaleski A J, Terekov A V, Rybaltchenko L F, Khristenko E V and Ishchenko L A 2009 *Low Temp. Phys.* **35** 517
[129] Ren Z A, Yang J, Lu W, Yi W, Che G C, Dong X L, Sun L L and Zhao Z X 2008 *Mater. Res. Innov.* **12** 105
[130] Yi W *et al* 2008 *Europhys. Lett.* **83** 57002
[131] Ren Z A *et al* 2008 *Chin. Phys. Lett.* **25** 2215
[132] Yang J *et al* 2008 *Supercond. Sci. Technol.* **21** 082001
[133] Fuchs G *et al* 2008 *Phys. Rev. Lett.* **101** 237003
[134] Ren Z A *et al* 2008 *Europhys. Lett.* **83** 17002
[135] Yang J *et al* 2008 *New J. Phys.* **11** 025005
[136] Wang C *et al* 2008 *Europhys. Lett.* **83** 67006
[137] Mu G, Zeng B, Zhu X, Han F, Cheng P, Shen B and Wen H H 2008 *Phys. Rev.* B **79** 104501
[138] Kasperkiewicz K, Bos J W G, Fitch A N, Prassides K and Margadonna S 2009 *Chem. Commun.* **6** 707
[139] Qi Y, Gao Z, Wang L, Wang D, Zhang X and Ma Y 2008 *Supercond. Sci. Technol.* **21** 115016
[140] Wang C, Jiang S, Tao Q, Ren Z, Li Y, Li L, Feng C, Dai J, Cao G and Xu Z 2009 *Europhys. Lett.* **86** 47002
[141] Li Y, Lin X, Zhou T, Shen J, Luo Y, Tao Q, Cao G and Xu Z 2009 doi:10.1016/j.saphysc.2009.11.014
[142] Cao G *et al* 2009 *Phys. Rev.* B **79** 174505
[143] Qi Y, Wang L, Gao Z, Wang D, Zhang X and Ma Y 2009 *Phys. Rev.* B **80** 054502
[144] Matsuishi S, Inoue Y, Nomura T, Hirano M and Hosono H 2008 *J. Phys. Soc. Japan* **77** 113709
[145] Wu G *et al* 2008 *J. Phys.: Condens. Matter* **21** 142203
[146] Cheng P, Shen B, Mu G, Zhu X, Han F, Zeng B and Wen H H 2009 *Europhys. Lett.* **85** 67003
[147] Jeevan H S, Hossain Z, Kasinathan D, Rosner H, Geibel C and Gegenwart P 2008 *Phys. Rev.* B **78** 092406
[148] Qi Y, Gao Z, Wang L, Wang D, Zhang X and Ma Y 2008 *New J. Phys.* **10** 123003
[149] Kasinathan D, Ormeci A, Koch K, Burkhardt U, Schnelle W, Jasper A L and Rosner H 2009 *New J. Phys.* **11** 025023
[150] Saha S R, Drye T, Kirshenbaum K, Butch N P and Paglione J 2010 *J. Phys.: Condens. Matter* **22** 072204
[151] Sefat A S, Jin R, Mcguire M M, Sales B C, Singh D J and Mandrus D 2008 *Phys. Rev. Lett.* **101** 117004
[152] Li L J *et al* 2009 *New J. Phys.* **11** 025008
[153] Ni N, Thaler A, Kracher A, Yan J Q, Budko S L and Canfield P C 2009 *Phys. Rev.* B **80** 024511
[154] Han F *et al* 2009 *Phys. Rev.* B **80** 024506
[155] Schnelle W, Leithejasper A, Gumeniuk R, Burkhardt U, Kasinathan D and Rosner H 2009 *Phys. Rev.* B **79** 214516
[156] Jiang S, Xing H, Xuan G, Wang C, Ren Z, Feng C, Dai J, Xu Z and Cao G 2009 *J. Phys.: Condens. Matter* **21** 382203
[157] Ren Z, Tao Q, Jiang S, Feng C, Wang C, Dai J, Cao G and Xu Z 2009 *Phys. Rev. Lett.* **102** 137002
[158] Parker D R, Pitcher M J, Baker P J, Franke I, Lancaster T, Blundell S J and Clarke S J 2009 *Chem. Commun.* **16** 2189
[159] Mizuguchi Y, Tomioka F, Tsuda S, Yamaguchi T and Takano Y 2009 *J. Phys. Soc. Japan* **78** 074712
[160] Ning F, Ahilan K, Imai T, Sefat A S, Jin R, Mcguire M A, Sales B C and Mandrus D 2009 *J. Phys. Soc. Japan* **78** 013711
[161] Sefat A S, Huq A, McGuire M A, Jin R, Sales B C and Mandrus D 2008 *Phys. Rev.* B **78** 104505
[162] Jasper A L, Schnelle W, Geibel C and Rosner H 2008 *Phys. Rev. Lett.* **101** 207004
[163] Kawabata A, Lee S C, Moyoshi T, Kobayashi Y and Sato M 2008 *J. Phys. Soc. Japan* **77** 147
[164] Li Y, Lin X, Tao Q, Wang C, Zhou T, Li L, Wang Q, He M, Cao G and Xu Z 2009 *New J. Phys.* **11** 053008
[165] Sato M, Kobayashi Y, Lee S C, Takahashi H, Satomi E and Miura Y 2010 *J. Phys. Soc. Japan* **79** 014710
[166] Kurmaev E Z, Wilks R G, Moewes A, Skorikov N A, Izyumov Y A, Finkelstein L D, Li R H and Chen X H 2008 *Phys. Rev.* B **78** 220503
[167] Felner I, Nowik I, Tsindlekht M I, Ren Z, Shen X, Che G and Zhao Z 2008 arXiv:0805.2794
[168] Nowik I, Jerusalem I F H U, Awana V P S, Vajpayee A and Kishan H 2008 *J. Phys.: Condens. Matter* **20** 292201
[169] Wu G, Chen H, Xie Y L, Yan Y J, Wu T, Liu R H, Wang X F, Fang D F, Ying J J and Chen X H 2008 *Phys. Rev.* B **78** 092503
[170] Awana V P S, Vajpayee A, Mudgel M, Kumar A, Meena R S, Tripathi R, Kumar S, Kotnala R K and Kishan H 2008 *J. Supercond. Novel Magn.* **21** 167
[171] Lu W, Yang J, Dong X L, Ren Z A, Che G C and Zhao Z X 2008 *New J. Phys.* **10** 063026
[172] Zhang H, Xu G, Dai X and Fang Z 2009 *Chin. Phys. Lett.* **26** 017401
[173] Lorenz B, Sasmal K, Chaudhury R P, Chen X H, Liu R H, Wu T and Chu C W 2008 *Phys. Rev.* B **78** 012505
[174] Zhao J *et al* 2008 *J. Am. Chem. Soc.* **130** 13828
[175] Kumai R, Takeshita N, Ito T, Kito H, Iyo A and Eisaki H 2009 *J. Phys. Soc. Japan* **78** 013705
[176] Lebgue S, Yin Z P and Pickett W E 2009 *New J. Phys.* **11** 025004
[177] Huang C, Chou C, Tseng K, Huang Y, Hsu F, Yeh K, Wu M and Yang H 2009 *J. Phys. Soc. Japan* **78** 084710
[178] Mizuguchi Y, Tomioka F, Tsuda S, Yamaguchi T and Takano Y 2008 *Appl. Phys. Lett.* **93** 152505
[179] Alireza P L, Ko Y T C, Gillett J, Petrone C M, Cole J M, Lonzarich G G and Sebastian S E 2009 *J. Phys.: Condens. Matter* **21** 012208
[180] Miclea C F, Nicklas M, Jeevan H S, Kasinathan D, Hossain Z, Rosner H, Gegenwart P, Geibel C and Steglich F 2009 *Phys. Rev.* B **79** 212509
[181] Kimber S A J *et al* 2009 *Nature Mater.* **8** 471
[182] He B, Dong C, Cao W, Liao C, Yang L and Chen H 2010 *Supercond. Sci. Technol.* **23** 025016
[183] Hunte F, Jaroszynski J, Gurevich A, Larbalestier D C, Jin R, Sefat A S, Mcguire M A, Sales B C, Christen D K and Mandrus D 2008 *Nature* **453** 903
[184] Senatore C, Cantoni M, Wu G, Liu R H, Chen X H and Flukiger R 2008 *Phys. Rev.* B **78** 054514
[185] Wang X, Ghorbani S R, Peleckis G and Dou S 2009 *Adv. Mater.* **21** 236

[186] Yuan H Q, Singleton J, Balakirev F F, Baily S A, Chen G F, Luo J L and Wang N L 2009 *Nature* **457** 565
[187] Fang M, Yang J, Balakirev F F, Kohama Y, Singleton J, Qian B, Mao Z Q, Wang H and Yuan H Q 2010 *Phys. Rev.* B **81** 020509
[188] Lee H, Bartkowiak M, Park J, Lee J, Kim J, Sung N, Cho B K, Jung C, Kim J S and Lee H 2009 *Phys. Rev.* B **80** 144512
[189] Ni N, Budko S L, Kreyssig A, Nandi S, Rustan G E, Goldman A I, Gupta S, Corbett J D, Kracher A and Canfield P C 2008 *Phys. Rev.* B **78** 014507
[190] Gurevich A 2003 *Phys. Rev.* B **67** 184515
[191] Gurevich A 2007 *Physica* C **456** 160
[192] Zhu X, Yang H, Fang L, Mu G and Wen H 2008 *Supercond. Sci. Technol.* **21** 105001
[193] Narduzzo A *et al* 2008 *Phys. Rev.* B **78** 012507
[194] Prakash J, Singh S J, Samal S L, Patnaik S and Ganguli A K 2008 *Europhys. Lett.* **84** 57003
[195] Jo Y *et al* 2009 *Physica* C **469** 566
[196] Fuchs G *et al* 2009 *New J. Phys.* **11** 075007
[197] Werthamer N R, Helfand E and Hohenberg P C 1966 *Phys. Rev.* **147** 295
[198] Braithwaite D, Lapertot G, Knafo1 W and Sheikin I 2010 *J. Phys. Soc. Japan* **79** 053703
[199] Lei H, Hu R, Choi E S, Warren J B and Petrovic C 2010 *Phys. Rev.* B **81** 094518
[200] Altarawneh M M, Collar K, Ni C H M N, Budko S L and Canfield P C 2008 *Phys. Rev.* B **78** 220505
[201] Baily S A, Kohama Y, Hiramatsu H, Maiorov B, Balakirev F F, Hirano M and Hosono H 2009 *Phys. Rev. Lett.* **102** 117004
[202] Blatter G, Feigelman M V, Geshkenbein V B, Larkin A I and Vinokur V M 1994 *Rev. Mod. Phys.* **66** 1125
[203] Zola D *et al* 2009 *J. Supercond. Novel Magn.* **22** 609
[204] Tarantini C, Gurevich A, Larbalestier D C, Ren Z, Dong X, Lu W and Zhao Z 2008 *Phys. Rev.* B **78** 184501
[205] Pust L, Kadlecova J, Jirsa M and Durcok S 1990 *J. Low Temp. Phys.* **78** 179
[206] Kwok W K, Fleshler S, Welp U, Vinokur V M, Downey J and Miller G W C M M 1992 *Phys. Rev. Lett.* **69** 3370
[207] Rydh A, Welp U, Hiller J M, Koshelev A E, Kwok W K, Crabtree G W, Kim K H P, Kim K H, Jung C U, Lee H S, Kang B and Lee S I 2003 *Phys. Rev.* B **68** 172502
[208] Wang X L, Ghorbani S R, Dou S X, Shen X, Yi W, Li Z and Ren Z 2008 arXiv:0806.1318
[209] Palstra T T M, Batlogg B, Dover R B V, Schneemeyer L F and Waszczak J V 1990 *Phys. Rev.* B **41** 6621
[210] Wanga X L, Li A H, Yu S, Ooi S, Hirata K, Lin C T, Collings E W, Sumption M D, Ding M B S Y and Dou S X 2005 *J. Appl. Phys.* **97** 10B114
[211] Sidorenko A, Zdravkov V, Ryazanov V, Horn S, Klimm S, Tidecks R, Wixforth A, Koch T and Schimme T 2005 *Phil. Mag.* **85** 1783
[212] Yang H, Ren C, Shan L and Wen H 2008 *Phys. Rev.* B **78** 092504
[213] Prakash J, Singh S J, Patnaik S and Ganguli A K 2009 *Physica* C **469** 82
[214] Kohama Y, Kamihara Y, Riggs S, Balakirev F F, Atake T, Jaime M, Hirano M and Hosono H 2008 *Europhys. Lett.* **84** 37005
[215] Kohama Y, Kamihara Y, Baily S A, Civale L, Riggs S C, Balakirev F F, Atake T, Jaime M, Hirano M and Hosono H 2009 *Phys. Rev.* B **79** 144527
[216] Yamamoto A *et al* 2009 *Appl. Phys. Lett.* **94** 062511
[217] Okazaki R *et al* 2009 *Phys. Rev.* B **79** 064520
[218] Ngo V T and Diep H T 2008 *J. Appl. Phys.* **103** 07C712
[219] Kametani F *et al* 2009 *Supercond. Sci. Technol.* **22** 015010
[220] Yamamoto A *et al* 2008 *Supercond. Sci. Technol.* **21** 095008
[221] Seuntjens J M and Larbalestier D C 1990 *J. Appl. Phys.* **67** 2007
[222] Moore J D *et al* 2008 *Supercond. Sci. Technol.* **21** 092004
[223] Yamamoto A *et al* 2008 *Appl. Phys. Lett.* **92** 252501
[224] Yang H, Luo H, Wang Z and Wen H 2008 *Appl. Phys. Lett.* **93** 142506
[225] Otabe E S *et al* 2009 *Physica* C **469** 1940
[226] Prozorov R, Tillman M E, Mun E D and Canfield P C 2009 *New J. Phys.* **11** 035004
[227] Prozorov R, Giannetta R W, Kameda N, Tamegai T, Schlueter J A and Fournier P 2003 *Phys. Rev.* B **67** 184501
[228] Kametani F *et al* 2009 *Appl. Phys. Lett.* **95** 142502
[229] Mcguire M A *et al* 2008 *Phys. Rev.* B **78** 094517
[230] Mu G, Zhu X, Fang L, Shan L, Ren C and Wen H 2008 *Chin. Phys. Lett.* **25** 2221
[231] Ding L, He C, Dong J K, Wu T, Liu R H, Chen X H and Li S Y 2008 *Phys. Rev.* B **77** 180510
[232] Mu G, Luo H, Wang Z, Ren Z, Shan L, Ren C and Wen H 2008 *Phys. Rev.* B **79** 174501
[233] Fukazawa H *et al* 2009 *J. Phys. Soc. Japan* **78** 083712
[234] Baker P J, Giblin S R, Pratt F L, Liu R H, Wu G, Chen X H, Pitcher M J, Parker D R, Clarke S J and Blundell S J 2009 *New J. Phys.* **11** 025010
[235] Gaudart L P and Dragoe N 2008 *J. Phys. Soc. Japan* **77** 58
[236] Matusiak M, Plackowski T, Bukowski Z, Zhigadlo N D and Karpinski J 2009 *Phys. Rev.* B **79** 212502
[237] Ricci A, Fratini M and Bianconi A 2009 *J. Supercond. Novel Magn.* **22** 305
[238] Lee C, Yin W and Ku W 2009 *Phys. Rev. Lett.* **103** 267001
[239] Sarun P M, Vinu S, Shabna R, Biju A and Syamaprasad U 2009 *J. Am. Ceram. Soc.* **92** 411
[240] Sarun P M, Shabna R, Vinu S, Biju A and Syamaprasad U 2009 *Physica* B **404** 1602
[241] Ovshinsky S R 2008 arXiv:0807.1673
[242] Guo L, Xue Y Y, Chen F, Xiong Q, Meng P L, Ramirez D, Chu C W, Eggert J H and Mao H K 1994 *Phys. Rev.* B **50** 4260
[243] Bianconi A 2000 *Int. J. Mod. Phys.* B **14** 3289
[244] Fratini M, Campi G, Barba L, Busby Y, Filippi M, Prellier W, Palmisano V, Simonelli L, Saini N L and Bianconi A 2007 *J. Supercond. Novel Magn.* **20** 551
[245] Fratini M, Campi G, Simonelli L, Palmisano V, Agrestini S, Filippi M, Saini N L and Bianconi A 2005 *J. Supercond.* **18** 71
[246] Boeri L, Dolgov O V and Golubov A A 2008 *Phys. Rev. Lett.* **101** 026403
[247] Shan L, Wang Y, Zhu X, Mu G, Fang L, Ren C and Wen H H 2008 *Europhys. Lett.* **83** 57004
[248] Bondino F *et al* 2008 *Phys. Rev. Lett.* **101** 267001
[249] Chen T Y, Tesanovic Z, Liu R H, Chen X H and Chien C L 2008 *Nature* **453** 1224
[250] Ren C, Wang Z S, Yang H, Zhu X Y, Fang L, Mu G, Shan L and Wen H H 2008 arXiv:0804.1726
[251] Machida Y, Tomokuni K, Isono T, Izawa K, Nakajima Y and Tamegai T 2009 *J. Phys. Soc. Japan* **78** 073705
[252] Mazin I I, Singh D J, Johannes M D and Du M H 2008 *Phys. Rev. Lett.* **101** 057003
[253] Millo O, Asulin I, Yuli O, Felner I, Ren Z, Shen X, Che G and Zhao Z 2008 *Phys. Rev.* B **78** 092505
[254] Jia Y, Cheng P, Fang L, Yang H, Ren C, Shan L, Gu C Z and Wen H H 2008 *Supercond. Sci. Technol.* **21** 105018
[255] Cvetkovic V and Tesanovic Z 2009 *Europhys. Lett.* **85** 37002
[256] Xu C and Sachdev S 2008 *Nature Phys.* **4** 898
[257] Norman M R 2008 *Physics* **1** 21
[258] Chubukov A 2009 *Physica* C **469** 640

#4

August 14, 2002

research news

A Most Unusual Superconductor and How It Works

First-principles calculation explains the strange behavior of magnesium diboride

Paul Preuss, (510) 486-6249, paul_preuss@lbl.gov

news releases
receive our news releases via email
science beat
lab home
lab a-z index
search
Advanced Search
Search Tips

BERKELEY, CA Magnesium diboride (MgB_2) becomes superconducting at 39 degrees Kelvin, one of the highest known transition temperatures (T_c) of any superconductor. What's more, its puzzling characteristics include more than one superconducting energy gap, a state of affairs anticipated in theory but never before seen experimentally.

Now theorists at Lawrence Berkeley National Laboratory and the University of California at Berkeley, led by Marvin Cohen and Steven Louie of Berkeley Lab's Materials Sciences Division, both professors of physics at UC Berkeley, have calculated the properties of this unique superconductor from first principles, revealing the secrets of its anomalous behavior. Collaborators in the project included postdoctoral fellow Hyoungjoon Choi, graduate student David Roundy, and visitor Hong Sun.

In the August 15 issue of *Nature*, the theorists report that MgB_2's odd features arise from two separate populations of electrons -- nicknamed "red" and "blue" -- that form different kinds of bonds among the material's atoms. As well as explaining conflicting observations, their calculations have led to predictions subsequently

born out by experiment. Further, they suggest the possibility of creating radically new materials with analogous electronic structure.

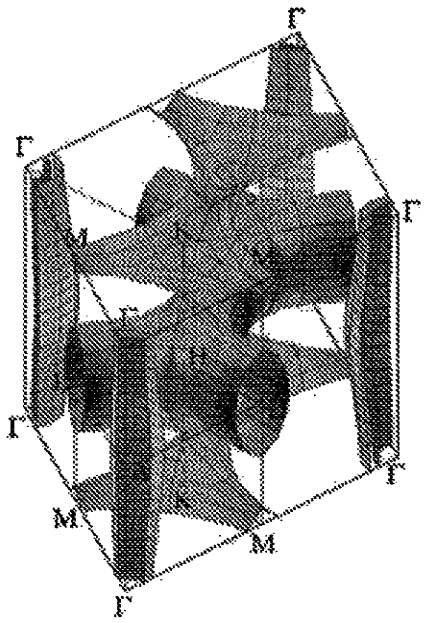

The size of superconducting energy gaps changes greatly on different sections of MgB2's complex Fermi surface.

Bottles of powdered MgB2 have been sitting on the chemical laboratory shelf since the 1950s, but not until January of 2001 did Japanese researchers announce their discovery that it was a relatively high-temperature superconductor. Like high-Tc superconductors made of cuprate ceramics, MgB2 is a layered material; while undoped cuprates are insulators at ordinary temperatures, however, MgB2 is always a metal.

"Structurally, magnesium diboride is almost as simple as pencil lead, graphite," says Louie. "It consists of hexagonal honey-combed planes of boron atoms separated by planes of magnesium atoms, with the magnesiums centered above and below the boron hexagons."

This remarkably simple atomic structure would eventually prove the key to understanding MgB2. But in the hundreds of papers produced in the first rush to examine the new superconductor, experimenters using different techniques found many different, unusual, and sometimes conflicting properties.

"It was like the blind men looking at the elephant," Cohen remarks. "Everybody who looked at MgB2

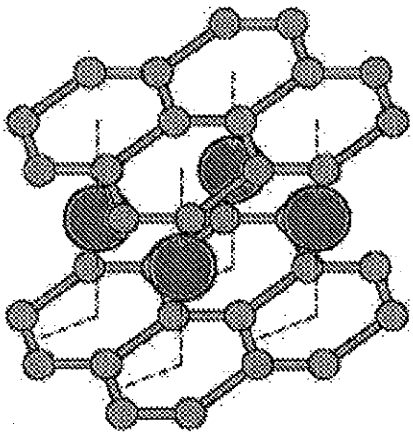

In MgB2, hexagonal honeycomb layers of boron atoms alternate with layers of magnesium atoms, centered on the hexagons.

saw a different picture. Some said the superconducting energy gap was this, others said it was that; still others found anomalies in measurements of specific heat."

It quickly became apparent that theories developed to explain superconductivity in the layered, high-Tc cuprates would not be helpful in understanding MgB2. Instead, Louie and Cohen and their colleagues used the well-established Bardeen-Cooper-Schrieffer (BCS) theory to examine the fundamental properties of MgB2, an effort made possible by a technique Choi developed to solve the BCS equations for materials with complex electronic structure.

"When we looked at the elephant," says Cohen, "we saw that almost everybody had been right!" The many different pictures were in fact consistent.

In BCS theory, electrons overcome their mutual repulsion to form pairs that can move through the material without resistance. Vital to pair formation are the quantized vibrations of the crystal lattice, known as phonons.

"Electrons pair by exchanging a phonon. If you think of a lattice of positive ions, you can picture them 'pulling' the electrons together into pairs, as vibration moves them toward passing electrons," says Cohen.

What was puzzling was that, in BCS theory, the coupling to the lattice required to form an electron pair should be equivalent to the coupling of a

single electron emitting and reabsorbing a phonon, giving rise to an enhanced electron mass. But in MgB2 these two values were apparently different -- a clue that more than one kind of electron might be involved in pairing. So the theorists began with basic considerations of MgB2's elemental constituents and layered structure.

"To understand the importance of crystal structure to MgB2's electronic states, compare it to graphite," Louie suggests. In the hexagonal planes of graphite, each carbon atom, which has four valence electrons, is bonded to three others, occupying all available planar bonding states, the sigma bonds; its remaining electron moves in orbitals above and below the plane, forming pi bonds.

MgB2, like graphite, has strong sigma bonds in the planes and weak pi bonds between them, but since boron atoms have fewer electrons than carbon atoms, not all the sigma bonds in the boron planes are occupied. And because not all the sigma bonds are filled, lattice vibration in the boron planes has a much stronger effect, resulting in the formation of strong electron pairs confined to the planes.

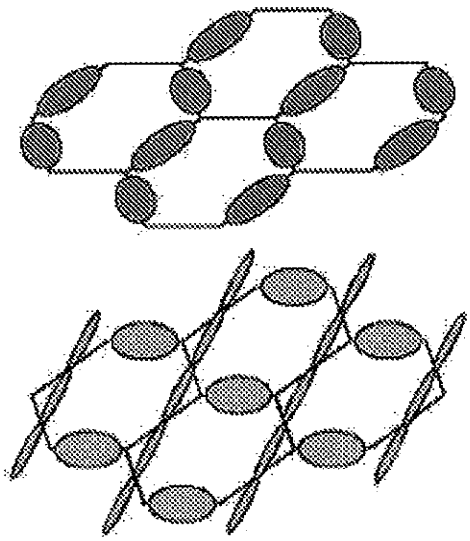

Strong sigma bonds lie in the plane. Not all sigma bonds in the boron layers of MgB2 are occupied.

"Partially occupied sigma bonds driving superconductivity in a layered structure is one of the new concepts that appeared from the

theoretical studies; generally speaking, nature does not like unoccupied sigma bond states," says Louie. "Our other major finding is that not all the boron electrons are needed in strong pair formation to achieve high Tc. In addition to the strongly bonded sigma pairs, the boron electrons involved in pi bonds form much weaker pairs."

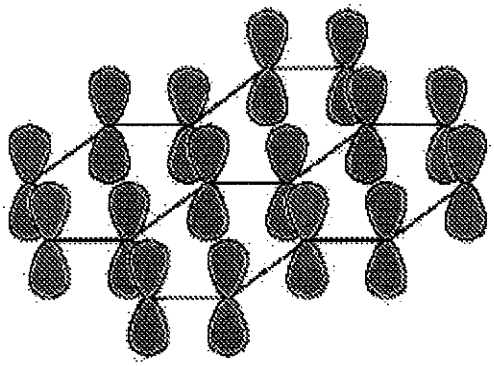

Weak pi bonds extend above and below the boron plane.

Stated differently, electrons on different parts of the Fermi surface form pairs with different binding energies. The theorists' graph of MgB2's extraordinary Fermi surface -- a way of visualizing the highest-energy states its electrons can occupy -- clearly shows the two populations of electrons and the different energies needed to break their superconducting pairs -- a graph that incidentally gives rise to the nicknames "red" and "blue" electrons.

Four distinctive kinds of sheets make up the Fermi surface (see first illustration, top). Two form nested cylinders: these map differently oriented sigma bonds and are colored orange and red to indicate the large amount of energy needed to break these superconducting pairs -- a large superconducting "gap," ranging from 6.4 to 7.2 thousandths of an electron volt (meV) at 4 degrees Kelvin.

Two other sheets of the Fermi surface form "webbed tunnels" and represent the pi-bonded electrons; they are colored green and blue to indicate the low energy (1.2 to 3.7 meV) required to break superconducting pairs of these electrons at 4 degrees K, constituting a separate superconducting gap.

The two kinds of electron pairs are coupled, and as temperature increases the superconducting gaps for "red" and "blue" pairs rapidly converge, until at about 39 degrees K both vanish. Above this temperature, all pairs are broken and the material does not superconduct.

The detailed theoretical calculations of the superconducting gaps and their temperature dependence for the "red" and "blue" electrons made it possible to interpret the experimental measurements, including those from scanning tunneling microscopy, optical studies, electron photoemission, and neutron analyses, and from heat capacity and infrared studies -- each a different way of "seeing the elephant."

Cohen and Louie and their colleagues performed their first-principles calculations on supercomputers at the Department of Energy's National Energy Research Scientific Computing Center (NERSC) based at Berkeley Lab and first shared them with the condensed-matter community last fall. Experimentalists have since confirmed many of the explicit predictions of their model. Among these was the existence of two superconducting gaps in MgB2, never before seen in any material.

Yet BCS theory contemplated the possibility of materials with multiple superconducting energy gaps early on, and the discovery of MgB2 raises the possibility that others could be made. Louie and Cohen have long studied the electronic properties of unusual materials incorporating boron, carbon, and nitrogen. MgB2 offers a new model for layered materials capable of high-temperature superconductivity.

"The origin of the anomalous superconducting properties of MgB2," by Hyoung Joon Choi, David Roundy, Hong Sun, Marvin L. Cohen, and Steven G. Louie, appears in the 15 August 2002 issue of Nature.

Berkeley Lab is a U.S. Department of Energy national laboratory located in Berkeley, California. It conducts unclassified scientific research and is managed by the University of California.

Additional information:
Download a PDF file of the *Nature* paper, "The origin of the anomalous superconducting properties of MgB2"

Of numerous experimental measurements of MgB2, many were performed by researchers at Berkeley Lab and the University of California at Berkeley. Two examples:

"Far-infrared optical conductivity gap in superconducting MgB2 films," by Kaindl, Carnahan, Orenstein, and Chemla, in collaboration with Christen, Zhai, Paranthaman, and Lowndes of Oak Ridge National Laboratory, *Physical Review Letters*, volume 88, number 2, 14 January 2002

"Specific heat of Mg^11B2: evidence for a second energy gap," by Bouquet, Fisher, and Phillips, in collaboration with Hinks and Jorgensen of Argonne National Laboratory, *Physical Review Letters*, volume 87, number 4, 23 July 2001

Hundreds of other papers on MgB2 from researchers worldwide